https://doi.org/10.1016/j.trb.2020.02.001

Ridesharing User Equilibrium Problem under OD-based Surge Pricing Strategy

Jie Ma [a,b], *Min Xu* [c], *Qiang Meng*[b,*], *Lin Cheng* [a]

[a]*School of Transportation, Southeast University, Nanjing 211189, China*

[b]*Department of Civil and Environmental Engineering, National University of Singapore, Singapore 117576, Singapore*

[c]*Department of Industrial and Systems Engineering, The Hong Kong Polytechnic University, Hung Hom, Hong Kong, China*

Abstract

Ridesharing is one of the effective urban traffic supply and demand management policies to reduce car ownership and mitigate traffic congestion. The origin-destination (OD) based surge pricing strategy is widely adopted by ridesharing service operators in practice due to its fairness and effectiveness. In this study, we aim to investigate the ridesharing user equilibrium (RUE) problem for an urban transportation network under the OD-based surge pricing strategy. We first build a variational inequality (VI) model for the proposed RUE problem. In particular, we explicitly formulate the necessary ride-matching constraints for the participants of multiple ridesharing services and rigorously demonstrate the existence and uniqueness of the RUE solution under some mild conditions. A parallel self-adaptive projection method (PSPM) incorporating column generation is developed to find an RUE solution for the large-scale problems. Finally, numerical experiments are conducted to provide valuable insights and examine the effectiveness of the proposed solution method. The results quantitatively show that the ridesharing under the OD-based surge pricing strategy reduces not only the travel cost for travelers but also the deliberate detours. Traffic congestion is significantly mitigated by ridesharing. Moreover, the proposed solution method has satisfactory computational efficiency for solving the large-scale problems.

Keywords: Ridesharing user equilibrium (RUE); OD-based pricing strategy; Ride-matching constraints; Variational inequality (VI); Parallel projection methods

1. Introduction

Shared mobility is touted to be one of the most promising innovations that reshape future urban mobility. As a notable example of shared mobility, ridesharing allows riders to travel with a less expense by sharing a ride with peer passengers, and it has been found to mitigate traffic congestion and reduce air pollution (Chan and Shaheen, 2012; Furuhata et al., 2013; Morency, 2007). These benefits and the advance of new communication technologies have led the fast development of ridesharing systems operated by commercial companies around the world (Amey, 2010; Masoud et al., 2017; Masoud and Jayakrishnan, 2017), which are referred to as transportation network companies (TNCs) hereafter. Examples include Uber in the United States, Didi in China, and Grab in Singapore.

The ultimate purpose of a ridesharing system is to aggregate travelers who share the same origin, destination, or partial path into one vehicle to reduce car use with an improved in-vehicle occupancy. There are multiple players involved in the ridesharing services, namely, solo drivers, ridesharing drivers, riders, and TNCs. The ridesharing drivers provide ridesharing services to the riders, while the solo drivers drive themselves without carrying any riders. A TNC functions as a ride-matching agent that pairs riders with ridesharing drivers, and it charges ridesharing price from riders, gives compensation to ridesharing drivers, and earns a profit from the difference. A traveler may freely switch the role among solo driver, ridesharing driver, as well as rider based on her/his own travel cost and benefit assessment. Therefore, the magnitude of ridesharing price and compensation would have significant impact on both supply (i.e., the number of ridesharing drivers) and demand sides (i.e., the number of riders), and thus affecting the sustainability and profitability of ridesharing services. For example, a low compensation may make no one willing to be a ridesharing driver so that the supply of ridesharing services will be insufficient. In contrast, a high ridesharing price will suppress ridesharing demand. How to set an appropriate ridesharing price and compensation is the critical issue faced by TNCs to achieve a sustainable ridesharing market.

Most TNCs set the surge or non-surge ridesharing price and compensation based on the travel time or distance of a path/trip (Campbell, 2018). Compared to the surge price, however, the non-surge price often results in a great more unfulfilled ridesharing requests especially at the peak demand period due to its limited ability to adjust supply and demand (Hall et al., 2015). Moreover, a path-dependent pricing strategy may prompt the ridesharing drivers to deliberately detour and travel on longer paths between an origin and destination (OD) pair to earn more compensation (Catriona, 2016). This phenomenon has been frequently complained by customers and negatively affects the operations of TNCs (RideGuru, 2018). The OD-based surge pricing strategy, i.e., setting the path-independent price based on the supply and demand between an OD pair, seems an inevitable approach to address the above issues. In fact, Grab in Singapore has been using an OD-based surge pricing strategy to attract customers (Grab, 2018).

The implementation of ridesharing services into an urban transportation network would affect the behaviors of travelers and in turn the user equilibrium (UE) traffic flow pattern. The interactions among the three key players, i.e., solo drivers, ridesharing drivers, as well as riders, create difficulty in solving the UE problem for an urban transportation network with ridesharing services, referred to as the ridesharing user equilibrium (RUE) problem, by those conventional models and solution methods. For example, in the traditional UE problem, a UE traffic flow pattern is restricted by traffic demand and transport infrastructure, while in the RUE the number of ridesharing drivers between an OD pair limits the number of riders. Besides, travel cost experienced by these three players in the RUE is heterogeneous and mutually affected. In other words, the solo drivers mainly consider their travel times, while the riders and ridesharing drivers incur additional ridesharing prices and compensations respectively plus the inconvenience cost of sharing a ride. The travel times between an OD pair depend on the number of solo drivers and ridesharing drivers, while the ridesharing price and the compensation are determined by the flow of ridesharing participants, i.e., ridesharing drivers and riders. Solving the RUE problem is essential for traffic flow forecast and traffic management policy assessment with ridesharing services. Therefore, this study focuses on model development and algorithm design for the RUE problem by considering the unique characteristics of ridesharing.

1.1 Literature review

Over the past decades, many studies have investigated the ridesharing systems from different aspects. The relevant research topics include the morning commute problems (Liu and Li, 2017; Ma and Zhang, 2017; Wang et al., 2019), travel reliability problems (Long et al., 2018), pricing strategy design (Liu and Li, 2017; Wang et al., 2018), ride-matching algorithm design (Masoud and Jayakrishnan, 2017), and user equilibrium problems (Di et al., 2018; Xu et al., 2015; Yan et al., 2019). For example, Liu and Li (2017) proposed a bottleneck model to examine the pricing scheme design of the ridesharing program in the morning commute. Ma and Zhang (2017) formulated a continuous-time dynamic ridesharing model for a single bottleneck corridor to study the morning commute problem with ridesharing services and dynamic parking charges. Long et al. (2018) proposed a stochastic ride-sharing model to investigate the effects of travel time uncertainty on travel reliability and travelers' generalized travel cost. To assess the impacts of cost-sharing strategies on the ridesharing program, Wang et al. (2018) put up a variational inequality (VI) model for the mode choices of heterogeneous travelers with continuously distributed values of time in a single-corridor network. Masoud and Jayakrishnan (2017) discussed the features of a peer-to-peer (P2P) ridesharing system and proposed an interesting ride-matching algorithm. Xu et al. (2015) formulated a link-based complementarity problem (CP) for the RUE problem. Di et al. (2018) further extended the work of Xu et al. (2015) by considering the network design problem (NDP) with ridesharing services to explore whether existing roads should be retrofitted into high-occupancy toll (HOT) lanes. Yan et al. (2019) considered the stochasticity of the travel cost and extended the RUE problem into the stochastic RUE problem.

The RUE problem, though important, has received limited attention due to its challenge in model building and algorithm design. To the best of our knowledge, only Di et al. (2018; 2017) and Xu et al. (2015) have ever investigated the RUE problem. Xu et al. (2015) proposed a link-based CP for the RUE problem using a link flow based cost function. Di et al. (2017) considered a more realistic cost function by incorporating a path-based occupancy ratio. Di et al. (2018) extended their model to a link-node formulation as the lower-level model of their NDP. Regrettably, the aforementioned studies assumed that ridesharing prices and compensations are path-dependent, which may not align with reality. On the one hand, most TNCs inform riders the ridesharing prices before the start of a trip such that riders can freely make their choice regarding whether they will take the ride by paying such price. Hence, from the aspect of TNCs, setting the ridesharing price and compensation based on link/path flow, which is unknown before the start of a trip, is hard to implement and control in practice. On the other hand, adopting a path-dependent pricing strategy would incur a high complaint rate for deliberate detours. Instead, the path-independent OD-based surge pricing strategy is more realistic and favorable. However, no study investigates the RUE problem with the practical OD-based ridesharing pricing strategy. Moreover, the proposed link-based models are inapplicable because of the non-additivity of ridesharing prices and compensations determined by the OD-based surge pricing strategy.

In another line of study, Daganzo (1981) developed the first equilibrium model for carpooling that can be regarded as an RUE prototype. As an extension, Xiao et al. (2016) investigate a morning commute problem with carpooling behavior under parking space constraint at destination. Nevertheless, the assumptions made by these two works are quite stringent and unsuitable for the ridesharing services (Di et al., 2018). The carpooling equilibrium does not explicitly formulate the flow and cost of riders; therefore, the riders' switching behavior is not considered. Moreover, since the in-vehicle occupancy of carpooling vehicles is assumed to be constant (usually as one or infinite riders per carpooling vehicle), the capacity for carrying riders are not taken into account by these studies. To tackle the above issues, Xu et al. (2015) and Di et al. (2018; 2017) formulated the capacity constraint as *side constraints*: upper and lower bounds constrained the riders, and the flow, cost, as well as switching behavior of riders were incorporated. However, the formulation of the side constraints entails the following stringent assumptions:

- All ridesharing vehicles must have the same capacity in carrying riders. In other words, the vehicles with different capacities are not allowed, which dramatically reduces the applicability of the existing RUE models.

- The integrity of seats and riders is not explicitly considered. Since the side constraints only constrain the upper and lower bounds for riders, the existing model may generate a solution with some ridesharing vehicles taking a fractional number of riders, which is unrealistic.
- The existing RUE model can generate only the average number of the riders and the occupancy ratio over each link or path, e.g., each ridesharing vehicle carries 1.5 riders on average on a specific link. An explicit flow pattern should include the flows of the solo drivers, the ridesharing drivers carrying one rider, the ridesharing drivers carrying two riders, etc.
- Only the very basic ridesharing service is considered. The existing RUE models are inapplicable to consider multiple types of ridesharing services. Specifically, the existing RUE models assume that the ridesharing drivers (riders) are homogeneous and provide (receive) only one type of ridesharing service. Thus, the ridesharing services that share a specific number of seats or with different prices and compensations are not described, e.g., the UberX service provided by Uber, the KuaiChe service provided by Didi, and the GrabCar service provided by Grab.

Besides the model development for the RUE problem, designing an effective solution method is also challenging. There are a few solution methods for solving the VI problems, including the proximal point method (Han et al., 2015), the alternating direction method (Chen et al., 2011), the Newton's method (Dial, 1997), the interior point method (Ferris and Pang, 1997), and the projection method (He et al., 2009; Levitxn, and Polyak, 1966). The projection method is recognized as a very effective way to solve the large-scale problems because of its small amount of computation in each iteration. Only the projection to the feasible set and some functions are needed. Several projection-type methods were thus proposed to solve the VI problems. Among them, the basic projection method was proposed by Goldstein (1964) and Levitxn and Polyak (1966). To calculate the step size, however, the basic projection method depends on the coercive modulus in advance, which is unknown in practice. Many studies are thus devoted to tackling this issue. For example, He et al. (2009) proposed a self-adaptive projection method that provides a self-adaptive step size search procedure by checking the Armijo's rule (Armijo, 1966) without the aid of the coercive modulus. However, for the large-scale problems, the projection-type methods may still need a large number of computational resources such as large in-memory requirement and computing time when calculating the projection.

1.2 Objective and contributions

The objective of this study is to close the identified research gap by developing a path-based VI model and a parallel self-adaptive projection method (PSPM) for the RUE problem under the OD-based surge pricing strategy. The main contributions of this study are listed as follows:

- We make the first attempt to incorporate the OD-based surge pricing strategy into the RUE problem. The ridesharing prices and compensations determined by the OD-based surge pricing strategy are easy to implement because once a rider puts a request from an origin to a destination, the TNCs can set a ridesharing price instantly based on the present supply and demand between that OD pair. In addition, since the ridesharing prices and compensations are the same on different paths between an OD pair, ridesharing drivers will be self-motivated to travel on shorter paths to save their cost, and riders will not be confronted by the detour issue. In this regards, the proposed OD-based surge pricing strategy is beneficial for the development of ridesharing and is expected to be favored by more and more TNCs.
- We propose a novel VI model with the ride-matching constraints for the RUE problem. The ride-matching constraints reflect the fact that the number of riders is subject to the numbers of ridesharing vehicles and seats. The necessary assumptions required by the side constraints used by the existing RUE models are relaxed, and multiple ridesharing services can be thus described by the proposed VI model. The multipliers associated with the ride-matching constraints are regarded as the *subsidies* and *premiums* besides the regular ridesharing prices and compensations. Moreover, the existence and uniqueness of the solution to the proposed VI model are demonstrated under mild assumptions.

- We propose a PSPM integrating column generation for solving the RUE problem. We use the techniques of column generation and parallel computing to improve the original self-adaptive projection method proposed by He et al. (2009) for large-scale problems. The proposed solution method can find a globally optimal solution and has satisfactory computational feasibility and efficiency. Both the computational time and the in-memory requirement are significantly reduced for large-scale RUE problems.
- Three networks, i.e., Braess network, Sioux-Falls network, and Eastern-Massachusetts network, are used to carry out the numerical experiments. We first use the Braess network to analyze the impact of ridesharing and perform sensitivity analysis to acquire important insights. The Sioux-Falls network and the Eastern-Massachusetts network are adopted to evaluate the computational feasibility and efficiency of the proposed solution method. The results show that the ridesharing under the OD-based surge pricing strategy can reduce deliberate detours, mitigate traffic congestion, and reduce travel costs for travelers.

The remainder of this study is organized as follows. In addtion to presenting the necessary notations and assumptions used for model building, the RUE problem with the OD-based surge pricing strategy is elaborated in Section 2. Section 3 formulates a VI model for the proposed RUE problem. We further demonstrate the existence and uniqueness of the RUE solution under some mild conditions. Section 4 develops the PSPM incorporating column generation for solving the VI model. Numerical experiments are conducted in Section 5. Section 6 concludes this study and proposes future research directions.

2. Notations, Assumptions, and Problem Statement

This section will introduce the following fundamentals for the RUE problem: ridesharing network, ride-matching constraints, OD-based supply and demand constraints, and generalized travel cost functions. For the sake of better readability, the notations used throughout this study are listed in Appendix A.

Let $G = (N, A)$ be an urban transportation network with the ridesharing services, i.e., a ridesharing network, where N is the set of nodes and A is the set of links. Let W be a set of origin-destination (OD) pairs, P^w be the set of all the acyclic paths connecting OD pair $w \in W$, and $q^w > 0$ be the travel demand between OD pair $w \in W$. In the ridesharing network, the travelers are divided into three groups: solo drivers, ridesharing drivers, and riders denoted by the sets of SD, RD, and R, respectively. As mentioned before, ridesharing drivers and riders are the ridesharing participants who should travel together. However, the solo drivers do not share their rides. Moreover, each group may contain multiple roles that are denoted by $i \in I = SD \cup RD \cup R$. Each role represents the participants for a specific type of ridesharing service. For instance, if we assume each ridesharing driver can take at most two riders, the three groups are divided into five roles: $i = 1 \in SD$ denotes the solo drivers; $i = 2{,}3 \in RD$ denote the ridesharing drivers providing 1-rider and 2-rider ridesharing services, i.e., the ridesharing drivers with one rider and two riders, respectively; and $i = 4{,}5 \in R$ denote the riders taken by the drivers $i = 2{,}3$, respectively. We consider the fixed travel demand between an OD pair, and assume that these travelers in ridesharing networks can choose their roles at the beginning of their trips to minimize their travel costs. Particularly, if it is not beneficial for a traveler to share rides, she/he will still travel as a solo driver. Let $f_{p,i}^w$ denote the path flow of the role i on path $p \in P^w$; the traffic flow conservation equations can be presented as follows:

$$\begin{cases} \sum_p \sum_i f_{p,i}^w = q^w, \forall w \\ f_{p,i}^w \geq 0, \forall w, \forall p, \forall i \end{cases} \tag{1}$$

Without loss of generality, we assume that the link travel time function $t_a(x_a)$, $a \in A$ is strictly monotone increasing with respect to link flow denoted by x_a. Among the three ridesharing players, the flows of solo drivers and the ridesharing drivers constitute the link flow, while riders cannot contribute to link flows because stay in vehicles share with ridesharing drivers. Let $x_{a,i}$ denote the flow of role i on link a, we thus have:

$$x_a = \sum_{i \in SD \cup RD} x_{a,i}, \forall a \in A \tag{2}$$

$$x_{a,i} = \sum_w \sum_p \delta^w_{a,p} f^w_{p,i}\,, \forall i \in SD \cup RD \cup R \quad (3)$$

where $\delta^w_{a,p} = 1$ if link a belongs to path p, otherwise $\delta^w_{a,p} = 0$. We let the vector $\mathbf{f} = (f^w_{p,i}, p \in P^w, w \in W, i \in I)^{\mathrm{T}}$ denote the path flows of all roles and $\mathbf{x} = (x_a, a \in A)^{\mathrm{T}}$ denote the link flow hereafter.

2.1 Ride-matching constraints

In the ridesharing network, the number of shared seats restricts the number of riders. This constraint has been formulated by Di et al. (2017) and Xu et al. (2015) as the side constraints:

$$f^w_{p,rd} \leq f^w_{p,r} \leq C f^w_{p,rd} \quad (4)$$

where $f^w_{p,r}$ and $f^w_{p,rd}$ denote the path flows of riders and ridesharing drivers on path p, respectively; and C denotes the capacity of a ridesharing vehicle, i.e., the number of seats.

However, the side constraints require stringent assumptions. Instead of using the side constraints, we can define a series of ride-matching constraints below for each class of ridesharing participants to describe the restriction of shared seats:

$$f^w_{p,\mathcal{T}_r(i)} = N_i \cdot f^w_{p,i}, \forall w, \forall p, \forall i \in RD \quad (5)$$

where $\mathcal{T}_r(i)$ maps the ridesharing driver $i \in RD$ to his/her riders $i' \in R$, i.e., $\mathcal{T}_r: RD \to R$; and the integer N_i is the number of seats shared by the ridesharing driver i. For instance, if $i = 2{,}3 \in RD$, which denote the 1-rider and 2-rider ridesharing drivers, respectively, we have $\mathcal{T}_r(2) = 4, \mathcal{T}_r(3) = 5$ representing the riders taken by the drivers $i = 2{,}3$, and accordingly $N_2 = 1$ and $N_3 = 2$ denoting the numbers of seats shared by the drivers $i = 2{,}3$, respectively. Therefore, each type of ridesharing driver is matched with a corresponding integer number of riders. The above constraints actually help us classify the ridesharing drivers and riders into more detailed categories. Thus, each type of ridesharing driver can have the different capacity in carrying riders; the integrity of riders and seats is considered; multiple ridesharing services that share a specific number of seats can be described; and a more explicit flow pattern is thus possible. Moreover, the matching constraints expressed by Eq. (5) can be easily modified for the multi-hop behavior that allows the drivers to pick up riders en route. Specifically, incorporating the technique of existing RUE models (Di et al., 2018; Xu et al., 2015), the ride-matching constraints in the context of multi-hop behavior is given by

$$x_{a,\mathcal{J}_r(i)} = N_i x_{a,i}, \forall a, \forall i \in RD \tag{6}$$

The riders can thus transfer from one ridesharing vehicle to another, and the riders in the same ridesharing vehicle do not necessarily have the same OD pair.

2.2 OD-based supply and demand constraints

In practice, the supply and demand of ridesharing services are inherently based on OD flows. For the sake of presentation, we define the OD-based ridesharing supply (i.e., the number of ridesharing drivers) and demand (i.e., the number of riders) as follows:

$$\begin{cases} s_i^w = \sum_p f_{p,i}^w \\ d_{\mathcal{J}_r(i)}^w = \sum_p f_{p,\mathcal{J}_r(i)}^w \end{cases}, \forall w, \forall i \in RD \tag{7}$$

The OD-based supply and demand are more reasonable than current measurements in literature, e.g., the link or path flows. This is because (i) the ridesharing requests proposed by the participants are often OD-oriented; (ii) the OD flows are much easier to collect compared with link or path flows; and (iii) the TNCs always use OD flows to measure the supply and demand in practice (Hall et al., 2015). Besides, since the OD flow is a summation of path flows, combining Eqs. (5) and (7) yields that:

$$d_{\mathcal{J}_r(i)}^w = N_i s_i^w, \forall w, \forall i \in RD \tag{8}$$

2.3 Generalized travel cost functions for solo drivers, ridesharing drivers and riders

As mentioned before, the three players' travel costs are heterogeneous and dependent. We classify their costs as follows: travel time cost, inconvenience cost, ridesharing price and compensation, and miscellaneous cost. The solo drivers only suffer travel time cost, while ridesharing participants experience inconvenience cost, ridesharing price and compensation in addition to travel time cost. The travelers' travel time cost depends on the flows of drivers, while the inconvenience cost, the price and the compensation are related to the flows of ridesharing participants.

Travel time cost

As we have discussed in the introduction, riders do not contribute to travel time cost: links become congested only because there are too many vehicles on roads. However, all the travelers experience travel time cost. Since the riders take ridesharing vehicles, they suffer the same travel time as the drivers do. Moreover, the values of time (VOTs) of the roles may be different. For instance, if the VOT of riders is lower than that of drivers, riders may lose less than the drivers do. Hence, we define the travel time cost for different roles as follows:

$$C_{p,i}^{T,w} \triangleq \rho_i t_p^w = \rho_i \sum_a \delta_{a,p}^w t_a(x_a), \forall w, p, i \tag{9}$$

where ρ_i denotes the VOT of each role i; t_p^w denotes the travel time on path p; and t_a denotes the travel time on link a. Note that the VOTs of roles are a little different from the VOTs of travelers in TAPs with public transit which usually indicate low incomes. Specifically, since the travelers in ridesharing are peers, there are no evidence that riders' income is lower. The VOT of riders is lower than that of drivers in RUE problems only because riders need not drive or pay attention to the traffic during their trips. They can do their own business, such as reading or listening to music, which create extra value for themselves and reduce their cost during the travel time.

Inconvenience cost

Only ridesharing drivers and riders may suffer inconvenience cost. The inconvenience cost derives from the discomfort of sharing rides with strangers. Different numbers of in-vehicle strangers may lead to different amounts of inconvenience cost. Hence, we define the inconvenience cost for each role $i \in RD \cup R$. Moreover, the longer the participants travel with strangers, the more inconvenience cost they experience. It is thus reasonable to assume that the inconvenience cost is related to the travel time, namely:

$$C_{p,i}^{I,w} \triangleq I_i\left(t_p^w\right), \forall w, p, \forall i \in RD \cup R \tag{10}$$

where $C_{p,i}^{I,w}$ represents the inconvenience cost for role i on path p and $I_i(\cdot)$ is a monotone increasing function with respect to travel time t_p^w. The inconvenience costs unrelated to travel time in other RUE studies can be regarded as a special case where the travel time is considered as a constant.

Ridesharing price and compensation

Many TNCs use surge prices and compensations to cater for the imbalance between ridesharing supply and demand. For instance, when there are more riders, they charge a high price and give ridesharing drivers a high compensation to incent the supply. Besides, a base price (compensation) should be set up to avoid the extremely low price (compensation). Thus, the ridesharing price (compensation) consists of two parts: base price and surge price. Moreover, some TNCs notice that the path-dependent prices motivate the ridesharing drivers to deliberately detour for more compensations (Catriona, 2016; RideGuru, 2018). To reduce the complaints caused by the detours, more and more TNCs are adopting path-independent OD-based surge pricing strategies (Grab, 2018). This study considers the OD-based surge pricing strategy defined by:

$$C_i^{M,w} \triangleq \begin{cases} -\left(B_i^w - C_i(s_i^w) + R_i\left(d_{\mathcal{T}_r(i)}^w\right)\right), \forall w, \forall i \in RD \\ B_i^w - C_i\left(s_{\mathcal{T}_{rd}(i)}^w\right) + R_i(d_i^w), \forall w, \forall i \in R \end{cases} \tag{11}$$

where $\mathcal{T}_{rd}(i)$ maps the rider $i \in R$ to his/her ridesharing driver $i' \in RD$, i.e., $\mathcal{T}_r: R \to RD$; When $i \in RD$, $C_i^{M,w}$ denotes the ridesharing compensations; when $i \in R$, $C_i^{M,w}$ denotes the ridesharing prices; B_i^w denotes the benchmark price (compensation) which is a base price (compensation) for each rider (ridesharing driver); $C_i(\cdot)$ and $R_i(\cdot)$ are monotone increasing functions with respect to the ridesharing supply and demand, respectively. $C_i(\cdot)$ and $R_i(\cdot)$ calculate the surge price or compensation for role i. Because of Eq. (8), the supply and demand have a closed-form relationship. The supply is a function with respect to the demand, and vice versa. We hence combine the functions $C_i(\cdot)$ and $R_i(\cdot)$, then Eq. (11) is equivalent to

$$C_i^{M,w} \triangleq \begin{cases} -\left(B_i^w - M_i(s_i^w)\right), \forall w, \forall i \in RD \\ B_i^w + M_i(d_i^w), \forall w, \forall i \in R \end{cases} \tag{12}$$

where $M_i(\cdot)$ is a monotone increasing function and calculates the surge prices or compensations for role i. Note that since $M_i(\cdot)$ is a function, the sign before $M_i(\cdot)$ actually does not matter, and $M_i(\cdot)$ is not necessarily positive or negative for any role i. We use these signs only to guarantee that the price $B_{i\in R}^w + M_{i\in R}(d_{i\in R}^w)$ is an increasing function with respect to $d_{i\in R}^w$ and the absolute value of the compensation $B_{i\in RD}^w - M_{i\in RD}(s_{i\in RD}^w)$ is a decreasing function with respect to $s_{i\in RD}^w$, which is the requirement of surge pricing strategies. Since the profit of TNCs comes from the difference between the ridesharing prices and the compensations, it is reasonable to assume that

$$N_i\left(B_{\mathcal{J}_r(i)}^w + M_{\mathcal{J}_r(i)}\left(d_{\mathcal{J}_r(i)}^w\right)\right) \geq B_i^w - M_i(s_i^w), \forall w, \forall i \in RD \tag{13}$$

Miscellaneous cost

The miscellaneous costs are classified into fixed costs and trip costs. The fixed costs include the costs of depreciation and insurance, and the trip costs include the fuel costs, parking costs, tolls, and other costs incurred during the trips. Since the travelers in ridesharing are peers who possess vehicles, they all bear the fixed costs which are sunk costs to ridesharing and do not affect the route and role choices. Thus, we omit the fixed costs when investigating the RUE problem. However, the trip costs are generated during the trips and are borne only by the drivers. We let c_t denote the trip costs hereafter. To sum up, the path travel cost functions are given by

$$C_{p,i}^w \triangleq \begin{cases} \rho_i t_p^w + c_t, \forall w, \forall p, \forall i \in SD \\ \rho_i t_p^w + I_i\left(t_p^w\right) - \left(B_i^w - M_i(s_i^w)\right) + c_t, \forall w, \forall p,\ \forall i \in RD \\ \rho_i t_p^w + I_i\left(t_p^w\right) + \left(B_i^w + M_i(d_i^w)\right), \forall w, \forall p, \forall i \in R \end{cases} \tag{14}$$

Subsidy and premium

According to the market clearance in economics, the ride-matching constraints describe only the actual supply and demand of the ridesharing services, while the potential supply and demand (if any) are suppressed by additional costs. Many studies on the traditional UE problem with link capacity constraints also considered such additional costs, and these costs were defined as the link tolls (Beckmann and Golob, 1974) and queueing delay time (Meng et al., 2008) and were incorporated into the generalized travel costs. In the proposed RUE problem, the generalized travel costs should also take into account the additional costs whose values should equal the relevant optimal Lagrangian multipliers associated with the ride-matching constraints (Patriksson, 2015). Otherwise, the supply and demand will be imbalanced. We thus define the subsidy and premium in the ridesharing system as follows:

$$\eta_{p,i}^{w} \triangleq \begin{cases} N_i \lambda_{p,i}^{w}, \forall w, \forall p, \forall i \in RD \\ -\lambda_{p,\mathcal{T}_{rd}(i)}^{w}, \forall w, \forall p, \forall i \in R \end{cases} \tag{15}$$

where $\lambda_{p,i}^{w}$ is the Lagrangian multiplier associated with the ride-matching constraint. When $\lambda_{p,i}^{w}$ is positive, $\eta_{p,i\in R}^{w}$ would be negative, representing a discount in the price for riders, while $\eta_{p,i\in RD}^{w}$ is positive, denoting an extraction from the compensation for ridesharing drivers. Conversely, when $\lambda_{p,i}^{w}$ is negative, $\eta_{p,i\in R}^{w}$ would be positive, denoting a premium price for riders, and $\eta_{p,i\in RD}^{w}$ is negative, representing a subsidy for ridesharing drivers.

In practice, the subsidy and premium $\eta_{p,i}^{w}$ can be regarded as one part of the surge prices and compensations. For instance, if there are more potential (not actual) riders $\mathcal{T}_r(i)$ than N_i times of the ridesharing drivers i on path p, the supply and demand of the N_i-rider ridesharing are imbalanced and the residual riders have to give up ridesharing or wait longer for being matched. In case of this, a negative multiplier $\lambda_{p,i}^{w}$ will be produced to balance the supply and demand. According to Eq. (15), a premium price $-\lambda_{p,i}^{w}$ will be charged by the TNC on the riders to cool the demand, and a subsidy of $N_i \lambda_{p,i}^{w}$ will be given to the ridesharing drivers to incent the supply since each ridesharing driver i serves N_i riders $\mathcal{T}_r(i)$. In contrast, if there is more potential supply than the demand, the positive $\lambda_{p,i}^{w}$ results in that a discount $-\lambda_{p,i}^{w}$ will be given to the riders and $N_i \lambda_{p,i}^{w}$ will be extracted from the compensations for ridesharing drivers.

In summary, the generalized path travel cost functions are given by

$$\tilde{C}_{p,i}^{w} \triangleq \begin{cases} \rho_i t_p^w + c_t, \forall w, \forall p, \forall i \in SD \\ \rho_i t_p^w + I_i(t_p^w) - \left(B_i^w - M_i(s_i^w)\right) + c_t + N_i \lambda_{p,i}^w, \forall w, \forall p,\ \forall i \in RD \\ \rho_i t_p^w + I_i(t_p^w) + \left(B_i^w + M_i(d_i^w)\right) - \lambda_{p,\mathcal{J}_{rd}(i)}^w, \forall w, \forall p, \forall i \in R \end{cases} \tag{16}$$

For instance, if we assume that ridesharing drivers can take at most two riders, the three ridesharing players will be divided into five roles: $i = 1 \in SD$ denotes the solo drivers; $i = 2,3 \in RD$ denote 1-rider and 2-rider ridesharing drivers, respectively; and $i = 4,5 \in R$ denote the riders taken by the ridesharing drivers $i = 2,3$, respectively. Then, the generalized travel cost functions for the above five roles are given by

$$\begin{cases} \tilde{C}_{p,1}^w = \rho_1 t_p^w + c_t \\ \tilde{C}_{p,2}^w = \rho_2 t_p^w + I_2(t_p^w) - \left(B_2^w - M_2(s_2^w)\right) + c_t + \lambda_{p,2}^w \\ \tilde{C}_{p,3}^w = \rho_3 t_p^w + I_3(t_p^w) - \left(B_3^w - M_3(s_3^w)\right) + c_t + 2\lambda_{p,3}^w, \forall w, p \\ \tilde{C}_{p,4}^w = \rho_4 t_p^w + I_4(t_p^w) + \left(B_4^w + M_4(d_4^w)\right) - \lambda_{p,2}^w \\ \tilde{C}_{p,5}^w = \rho_5 t_p^w + I_5(t_p^w) + \left(B_5^w + M_5(d_5^w)\right) - \lambda_{p,3}^w \end{cases} \tag{17}$$

Remark 1. For the case that the ridesharing vehicles may have more than two riders, the travelers can be classified into more roles. The generalized travel cost functions and the ride-matching constraints can be easily modified. Such problems are still within the framework of the proposed model.

Remark 2. For the case that some specific roles may have different VOTs, inconvenience coefficients, trip costs, etc., such roles can be further classified into sub-roles. The generalized travel cost functions and the ride-matching constraints can be easily modified. Such problems can still be addressed by the proposed methodology.

Compared with the traditional UE problem (Ban et al., 2012; Ma et al., 2018a; Sheffi, 1985), the proposed RUE problem has the following unique characteristics: (i) there are multiple types of travelers; (ii) the travel cost experienced by three players is heterogeneous and mutually affected; and (iii) the capacity in carrying riders is determined by the number of ridesharing drivers rather than traffic capacity in the traditional UE problems. These characteristics make the RUE to be an asymmetric problem that cannot be formulated as an ordinary multi-modal TAP or a mathematical programming model which can be solved by many efficient algorithms (e.g., Di et al., 2014). It is a challenge to formulate the RUE problem. In the traditional UE problem, travelers choose their routes to minimize their travel times. However, in the RUE problem, travelers can choose not only their routes but also their roles and the numbers of their peers to minimize their generalized travel costs. Specifically, the ride-matching constraints imply that the ridesharing drivers can further decide the number of seats they share, and the riders can choose whether to travel with other riders. Therefore, the RUE state is achieved if no one can reduce her/his generalized travel cost by unilaterally changing her/his route or role. In other words, at an RUE state, the generalized travel costs for all the used paths and all the roles are equal, and those for the unused paths are at least not lower than those for the used ones. This is a variant of the Wardrop first principle with the ridesharing services, which is referred to as the RUE principle.

3. Mathematical Model

According to the above description, we propose the mathematical formulation of the RUE principle:

$$\begin{cases} f_{p,i}^{w} > 0 \Rightarrow \tilde{C}_{p,i}^{w} = \pi^{w} \\ f_{p,i}^{w} = 0 \Rightarrow \tilde{C}_{p,i}^{w} \geq \pi^{w} \end{cases}, \forall p, \forall i, \forall w \tag{18a}$$

$$\sum_{p} \sum_{i} f_{p,i}^{w} - q^{w} = 0, \forall w \tag{18b}$$

$$N_i \cdot f_{p,i}^{w} - f_{p,\mathcal{I}_r(i)}^{w} = 0, \forall w, \forall p, \forall i \in RD \tag{18c}$$

Eq. (18a) can be rewritten as the complementarity constraints:

$$0 \leq f_{p,i}^{w} \perp \tilde{C}_{p,i}^{w} - \pi^{w} \geq 0, \forall p, \forall i, \forall w \tag{19}$$

where ⊥ is an orthogonal sign which makes the inner product of two vectors be zero. In what follows, we first build a VI model for the RUE principle and proceed to examine the existence and uniqueness of the RUE solution.

3.1 Variational inequality model

Let $\mathbf{\Psi}(\mathbf{f}) = (C_{p,i}^{w}, p \in P^{w}, w \in W, i \in I)^{\mathrm{T}}$ denote the vector of the travel cost function and Ω denote the set of feasible path flows, namely, $\Omega \triangleq \{\mathbf{f} | \text{Eqs.} (1) \text{ and } (5) \text{ are satisfied}\}$. It can be seen that $\mathbf{\Psi}: \Omega \subseteq \mathbb{R}^{|P||I|} \to \mathbb{R}^{|P||I|}$ where $P = \bigcup_{w} P^{w}$. Based on these notations, we present the VI model below:

[VI-RUE]: find a vector $\mathbf{f}^{*} \in \Omega$ such that

$$(\mathbf{f} - \mathbf{f}^{*})^{\mathrm{T}} \mathbf{\Psi}(\mathbf{f}^{*}) \geq 0, \forall\, \mathbf{f} \in \Omega \tag{20}$$

Proposition 1: Any solutions to the model [VI-RUE] fulfill the RUE principle.

Proof. Eq. (20) is clearly equivalent to

$$\mathbf{f}^{\mathrm{T}} \mathbf{\Psi}(\mathbf{f}^{*}) \geq \mathbf{f}^{*} \mathbf{\Psi}(\mathbf{f}^{*}), \forall\, \mathbf{f} \in \Omega \tag{21}$$

A vector $\mathbf{f}^{*}$ is a solution to the model [VI-RUE] if and only if $\mathbf{f}^{*}$ is a solution of the mathematical programming in the variable $\mathbf{f}$ (with $\mathbf{f}^{*}$ considered fixed):

$$\min_{\mathbf{f} \in \Omega} \mathbf{f}^{\mathrm{T}} \mathbf{\Psi}(\mathbf{f}^{*}) \tag{22}$$

The Karush-Kuhn-Tucker (KKT) condition for the mathematical programming (22) implies that

$$\begin{cases} 0 \leq f_{p,i}^{w} \perp \tilde{C}_{p,i}^{w} - \pi^{w} \geq 0 \\ \sum_{p} \sum_{i} f_{p,i}^{w} - q^{w} = 0, \forall w \\ N_{i} \cdot f_{p,i}^{w} - f_{p,\mathcal{T}_{r}(i)}^{w} = 0, \forall w, \forall p, \forall i \in RD \end{cases} \tag{23}$$

which is exactly the RUE principle. □

Note that although the mathematical programming (22) is the key to prove Proposition 1, it cannot be solved directly because its objective function involves the unknown solution $\mathbf{f}^{*}$ of the model [VI-RUE]. One may argue that since the multipliers $\lambda_{p,i}^{w}$ included in the ridesharing prices and compensations are based on paths, will they make the prices and compensations not OD-based? Defining the paths with positive ridesharing participants as the *used ridesharing paths*, we have the following propositions.

Proposition 2. The multipliers $\lambda_{p,i}^{w}$ are equal over all the used ridesharing paths $p \in P^{w}$ between OD pair w.

Proof. Without loss of generality, we assume p_1, p_2 are any two used ridesharing paths at the RUE state, i.e., $p_1, p_2 \in P^{w}$. According to Eq. (16), we have:

$$\lambda_{p,i}^{w} = \begin{cases} \frac{1}{N_i}\left(\tilde{C}_{p,i}^{w} - \rho_i t_p^{w} - I_i\left(t_p^{w}\right) - C_{p,i}^{M,w} - c_t\right) \\ \rho_{\mathcal{T}_r(i)} t_p^{w} + I_{\mathcal{T}_r(i)}(t_p^{w}) + C_{p,\mathcal{T}_r(i)}^{M,w} - \tilde{C}_{p,\mathcal{T}_r(i)}^{w} \end{cases} \forall p, \forall w, \forall i \in RD \tag{24}$$

Since $C_{p,i}^{M,w}$ is OD-based, i.e., $C_{p_1,i}^{M,w} = C_{p_2,i}^{M,w}$, $\forall i \in RD \cup R$, we have:

$$\lambda_{p_1,i}^{w} - \lambda_{p_2,i}^{w} = \begin{cases} \frac{1}{N_i}\left[\left(\tilde{C}_{p_1,i}^{w} - \tilde{C}_{p_2,i}^{w}\right) - \rho_i \cdot \left(t_{p_1}^{w} - t_{p_2}^{w}\right) - \left(I_i\left(t_{p_1}^{w}\right) - I_i\left(t_{p_2}^{w}\right)\right)\right] \\ \rho_{\mathcal{T}_r(i)}\left(t_{p_1}^{w} - t_{p_2}^{w}\right) + \left(I_{\mathcal{T}_r(i)}\left(t_{p_1}^{w}\right) - I_{\mathcal{T}_r(i)}\left(t_{p_2}^{w}\right)\right) - \left(\tilde{C}_{p_1,\mathcal{T}_r(i)}^{w} - \tilde{C}_{p_2,\mathcal{T}_r(i)}^{w}\right) \end{cases} \forall p, \forall w, \forall i \in RD \tag{25}$$

Since paths p_1 and p_2 are two used ridesharing paths at the RUE state, we have $\tilde{C}_{p_1,i}^{w} = \tilde{C}_{p_2,i}^{w}$, $\tilde{C}_{p_1,\mathcal{T}_r(i)}^{w} = \tilde{C}_{p_2,\mathcal{T}_r(i)}^{w}$. Therefore,

$$\lambda_{p_1,i}^{w} - \lambda_{p_2,i}^{w} = \begin{cases} \frac{1}{N_i}\left[-\rho_i \cdot \left(t_{p_1}^{w} - t_{p_2}^{w}\right) - \left(I_i\left(t_{p_1}^{w}\right) - I_i\left(t_{p_2}^{w}\right)\right)\right] \\ \rho_{\mathcal{T}_r(i)}\left(t_{p_1}^{w} - t_{p_2}^{w}\right) + \left(I_{\mathcal{T}_r(i)}\left(t_{p_1}^{w}\right) - I_{\mathcal{T}_r(i)}\left(t_{p_2}^{w}\right)\right) \end{cases}$$

$$\Rightarrow \left(\frac{1}{N_i}\rho_i + \rho_{\mathcal{T}_r(i)}\right) t_{p_1}^{w} + \frac{1}{N_i} I_i\left(t_{p_1}^{w}\right) + I_{\mathcal{T}_r(i)}\left(t_{p_1}^{w}\right) = \left(\frac{1}{N_i}\rho_i + \rho_{\mathcal{T}_r(i)}\right) t_{p_2}^{w} + \frac{1}{N_i} I_i\left(t_{p_2}^{w}\right) + I_{\mathcal{T}_r(i)}\left(t_{p_2}^{w}\right)$$

Define $\Phi(\cdot) \triangleq \left(\frac{1}{N_i}\rho_i + \rho_{\mathcal{T}_r(i)}\right) \times (\cdot) + \frac{1}{N_i} I_i(\cdot) + I_{\mathcal{T}_r(i)}(\cdot)$, since t_p^{w} and $I_i(\cdot)$ are both strictly monotone functions with respect to t_p^{w}, we know that $\Phi(\cdot)$ is also a strictly monotone function regarding t_p^{w}. Thus, $\Phi\left(t_{p_1}^{w}\right) = \Phi\left(t_{p_2}^{w}\right)$ implies that $t_{p_1}^{w} = t_{p_2}^{w}$, and then $\lambda_{p_1,i}^{w} = \lambda_{p_2,i}^{w}$. □

Proposition 3. The used paths (including ridesharing paths and non-ridesharing paths) between an OD pair must be the shortest in terms of travel time for all roles (if any) between the OD pair at the RUE state.

Proof. Without loss of generality, we assume p_1 is a used ridesharing path at the RUE state, $p_1 \in P^w$. According to Eq. (18a), the generalized travel cost $\tilde{C}^w_{p_1,i} = \pi^w$ is minimal by definition. Note that we cannot simply employ the conclusion for the traditional UE state or directly claim $t^w_{p_1} = C^w_{p_1,i}/\rho_i = \pi^w/\rho_i$ for solo driver $i \in SD$ to prove this proposition, since there may be no solo drivers but only ridesharing participants on some paths. We consider the following two cases.

Case 1. If there are solo drivers on the path p_1, the travel time has to be minimal, i.e., $t^w_{p_1} = \pi^w/\rho_{i\in SD} \leq t^w_p, \forall p \in P^w$. Otherwise, there must exist $\pi'^w < \pi^w$ making p_1 with no solo drivers on it.

Case 2. If there are no solo drivers on path p_1, path p_1 can only be a used ridesharing path. According to Proposition 2, the multipliers $\lambda^w_{p,i}$ are equal over all the used ridesharing paths. Thus, $\rho_i \times (\cdot) + I_i(\cdot) = \tilde{C}^w_{p_1,i} - C^{M,w}_{p_1,i} - \eta^w_{p_1,i}$ is minimal. Define $\Gamma_i(\cdot) \triangleq \rho_i \times (\cdot) + I_i(\cdot)$; then, $\Gamma_i(\cdot)$ is a strictly monotone increasing function with respect to travel time t^w_p. Therefore, $t^w_{p_1} = \Gamma_i^{-1}\left(\tilde{C}^w_{p_1,i} - C^{M,w}_{p_1,i} - \eta^w_{p_1,i}\right) \leq t^w_p, \forall p \in P^w$, i.e., the travel time on path p_1 is minimal for all roles.

The proof is thus completed. □

It should be pointed out that the above propositions indicate that ridesharing drivers seek the paths with minimal travel times under the OD-based pricing strategy. It implies that TNCs may reduce the complaints about deliberate detours if they use an OD-based pricing strategy (Catriona, 2016; RideGuru, 2018).

Proposition 4. A shortest path in terms of travel time between an OD pair is also a shortest path in terms of generalized travel cost for all roles between the OD pair.

Proof. Without loss of generality, we assume that p_1 is a shortest path in terms of travel time between a given OD pair. We only need to consider the following two cases.

Case 1. For solo drivers, since $\tilde{C}^w_{p_1,i} = \rho_i t^w_{p_1}, \forall w, \forall i \in SD$ where $\rho_i > 0$, p_1 is obviously the shortest path in terms of generalized travel cost.

Case 2. For ridesharing participants, we use the reduction to absurdity. Assume that p_1 is not the shortest path in terms of generalized travel cost, there must be other paths which are shortest. We consider two circumstances. Circumstance 1. If all these shortest paths carry no ridesharing participants, then it falls into Case 1. Circumstance 2. If there is at least one path p_2 that carries ridesharing participants, we have $\tilde{C}^w_{p_1,2} > \tilde{C}^w_{p_2,2}$, and $f^w_{p_2,3} > 0$. According to Proposition 3, p_2 is a used path and must also be a shortest path in terms of travel time, i.e., $t^w_{p_1} = t^w_{p_2}$. According to Eq. (16), we have $\lambda^w_{p_1,2} > \lambda^w_{p_2,2}$ which leads to $\tilde{C}^w_{p_1,3} < \tilde{C}^w_{p_2,3}$ and then $f^w_{p_2,3} = 0$ which contradicts with $f^w_{p_2,3} > 0$.

The proof is thus completed. □

3.2 Existence and uniqueness of the RUE solution

It is necessary to show the existence and uniqueness of the RUE solution based on the model [VI-RUE]. Since $\mathbf{\Psi}(\cdot)$ is continuous on the compact set Ω, the existence is immediate, and the proof of existence is thus omitted. We pay attention to the uniqueness.

Proposition 5. The model [VI-RUE] has a unique solution, namely, the path flow pattern is unique at the RUE state, if the following conditions hold:

(A) M_i is strictly monotone increasing, i.e., $\partial_i M_i > 0$

(B) $\rho_1 > \left(\sum_{i\in RD} \frac{(\rho_i + d_i - \rho_1)^2}{4\partial_i M_i} + \sum_{i\in R} \frac{(\rho_i + d_i)^2}{4\partial_i M_i}\right) \sum_a \delta^w_{a,p} \dot{t}_a$

where ρ_1 is the VOT of solo drivers; ∂_i denotes $\frac{d}{d\sum_p f^w_{p,i}}$; $\dot{t}_a$ denotes $\frac{dt_a(x_a)}{dx_a}$; and d_i denotes $\frac{dI_i(t^w_p)}{dt^w_p}$ for simplicity.

Proof. We first investigate the positive definiteness of Jacobian matrix **J** of $\boldsymbol{\Psi}(\cdot)$. For the sake of presentation, without loss of generality, we use the travel cost functions for five roles as an example to illustrate an explicit Jacobian matrix. The Jacobian matrix **J** of $\boldsymbol{\Psi}(\cdot)$ for this case is given by

$$\mathbf{J} = \begin{bmatrix} \frac{\partial C_{p,1}^{w}}{\partial f_{p,1}^{w}} & \frac{\partial C_{p,1}^{w}}{\partial f_{p,2}^{w}} & \frac{\partial C_{p,1}^{w}}{\partial f_{p,3}^{w}} & \frac{\partial C_{p,1}^{w}}{\partial f_{p,4}^{w}} & \frac{\partial C_{p,1}^{w}}{\partial f_{p,5}^{w}} \\ \frac{\partial C_{p,2}^{w}}{\partial f_{p,1}^{w}} & \frac{\partial C_{p,2}^{w}}{\partial f_{p,2}^{w}} & \frac{\partial C_{p,2}^{w}}{\partial f_{p,3}^{w}} & \frac{\partial C_{p,2}^{w}}{\partial f_{p,4}^{w}} & \frac{\partial C_{p,2}^{w}}{\partial f_{p,5}^{w}} \\ \frac{\partial C_{p,3}^{w}}{\partial f_{p,1}^{w}} & \frac{\partial C_{p,3}^{w}}{\partial f_{p,2}^{w}} & \frac{\partial C_{p,3}^{w}}{\partial f_{p,3}^{w}} & \frac{\partial C_{p,3}^{w}}{\partial f_{p,4}^{w}} & \frac{\partial C_{p,3}^{w}}{\partial f_{p,5}^{w}} \\ \frac{\partial C_{p,4}^{w}}{\partial f_{p,1}^{w}} & \frac{\partial C_{p,4}^{w}}{\partial f_{p,2}^{w}} & \frac{\partial C_{p,4}^{w}}{\partial f_{p,3}^{w}} & \frac{\partial C_{p,4}^{w}}{\partial f_{p,4}^{w}} & \frac{\partial C_{p,4}^{w}}{\partial f_{p,5}^{w}} \\ \frac{\partial C_{p,5}^{w}}{\partial f_{p,1}^{w}} & \frac{\partial C_{p,5}^{w}}{\partial f_{p,2}^{w}} & \frac{\partial C_{p,5}^{w}}{\partial f_{p,3}^{w}} & \frac{\partial C_{p,5}^{w}}{\partial f_{p,4}^{w}} & \frac{\partial C_{p,5}^{w}}{\partial f_{p,5}^{w}} \end{bmatrix} =$$

$$\begin{bmatrix} \rho_1 \sum_a \delta_{a,p}^{w} \dot{t}_a & \rho_1 \sum_a \delta_{a,p}^{w} \dot{t}_a & \rho_1 \sum_a \delta_{a,p}^{w} \dot{t}_a & 0 & 0 \\ (\rho_2 + d_2) \sum_a \delta_{a,p}^{w} \dot{t}_a & (\rho_2 + d_2) \sum_a \delta_{a,p}^{w} \dot{t}_a + \partial_2 M_2 & (\rho_2 + d_2) \sum_a \delta_{a,p}^{w} \dot{t}_a & 0 & 0 \\ (\rho_3 + d_3) \sum_a \delta_{a,p}^{w} \dot{t}_a & (\rho_3 + d_3) \sum_a \delta_{a,p}^{w} \dot{t}_a & (\rho_3 + d_3) \sum_a \delta_{a,p}^{w} \dot{t}_a + \partial_3 M_3 & 0 & 0 \\ (\rho_4 + d_4) \sum_a \delta_{a,p}^{w} \dot{t}_a & (\rho_4 + d_4) \sum_a \delta_{a,p}^{w} \dot{t}_a & (\rho_4 + d_4) \sum_a \delta_{a,p}^{w} \dot{t}_a & \partial_4 M_4 & 0 \\ (\rho_5 + d_5) \sum_a \delta_{a,p}^{w} \dot{t}_a & (\rho_5 + d_5) \sum_a \delta_{a,p}^{w} \dot{t}_a & (\rho_5 + d_5) \sum_a \delta_{a,p}^{w} \dot{t}_a & 0 & \partial_5 M_5 \end{bmatrix} \quad (26)$$

Since **J** is an asymmetric matrix whose positive definiteness cannot be proved by the methods for the symmetric matrices (Johnson, 1970), we construct a symmetric matrix and apply the third type of Gauss-Jordan operation to it:

$$\tilde{\mathbf{J}} = \mathbf{J} + \mathbf{J}^{\mathrm{T}} =$$

$$\begin{bmatrix} 2\rho_1 \sum_a \delta_{a,p}^w \dot{t}_a & (\rho_1+\rho_2+d_2)\sum_a \delta_{a,p}^w \dot{t}_a & (\rho_1+\rho_3+d_3)\sum_a \delta_{a,p}^w \dot{t}_a & (\rho_4+d_4)\sum_a \delta_{a,p}^w \dot{t}_a & (\rho_5+d_5)\sum_a \delta_{a,p}^w \dot{t}_a \\ (\rho_1+\rho_2+d_2)\sum_a \delta_{a,p}^w \dot{t}_a & 2(\rho_2+d_2)\sum_a \delta_{a,p}^w \dot{t}_a + 2\partial_2 M_2 & (\rho_2+\rho_3+d_2+d_3)\sum_a \delta_{a,p}^w \dot{t}_a & (\rho_4+d_4)\sum_a \delta_{a,p}^w \dot{t}_a & (\rho_5+d_5)\sum_a \delta_{a,p}^w \dot{t}_a \\ (\rho_1+\rho_3+d_3)\sum_a \delta_{a,p}^w \dot{t}_a & (\rho_2+\rho_3+d_2+d_3)\sum_a \delta_{a,p}^w \dot{t}_a & 2(\rho_3+d_3)\sum_a \delta_{a,p}^w \dot{t}_a + 2\partial_3 M_3 & (\rho_4+d_4)\sum_a \delta_{a,p}^w \dot{t}_a & (\rho_5+d_5)\sum_a \delta_{a,p}^w \dot{t}_a \\ (\rho_4+d_4)\sum_a \delta_{a,p}^w \dot{t}_a & (\rho_4+d_4)\sum_a \delta_{a,p}^w \dot{t}_a & (\rho_4+d_4)\sum_a \delta_{a,p}^w \dot{t}_a & 2\partial_4 M_4 & 0 \\ (\rho_5+d_5)\sum_a \delta_{a,p}^w \dot{t}_a & (\rho_5+d_5)\sum_a \delta_{a,p}^w \dot{t}_a & (\rho_5+d_5)\sum_a \delta_{a,p}^w \dot{t}_a & 0 & 2\partial_5 M_5 \end{bmatrix}$$

$$\xrightarrow{3-type\ Gauss-Jordan\ eliminations} \begin{bmatrix} 2\rho_1 \sum_a \delta_{a,p}^w \dot{t}_a - \left(\sum_{i=2}^{3} \frac{(\rho_i+d_i-\rho_1)^2}{2\partial_i M_i} + \sum_{i=4}^{5} \frac{(\rho_i+d_i)^2}{2\partial_i M_i}\right)\left(\sum_a \delta_{a,p}^w \dot{t}_a\right)^2 & 0 & 0 & 0 & 0 \\ 0 & 2\partial_2 M_2 & 0 & 0 & 0 \\ 0 & 0 & 2\partial_3 M_3 & 0 & 0 \\ 0 & 0 & 0 & 2\partial_4 M_4 & 0 \\ 0 & 0 & 0 & 0 & 2\partial_5 M_5 \end{bmatrix}$$

The 3-type Gauss-Jordan elimination does not change the positive definiteness of a matrix. By checking the determinants associated with all the up-left sub-matrices of $\tilde{\mathbf{J}}$, it can be seen that $\tilde{\mathbf{J}}$ is positive definite under Conditions (A) and (B).

According to the definition of positive definiteness, the matrix $\tilde{\mathbf{J}}$ is positive definite if and only if $\mathbf{x}^{\mathrm{T}}\tilde{\mathbf{J}}\mathbf{x} > 0$ for any non-zero vector $\mathbf{x}$, namely:

$$\mathbf{x}^{\mathrm{T}}\tilde{\mathbf{J}}\mathbf{x} = \mathbf{x}^{\mathrm{T}}\left(\mathbf{J} + \mathbf{J}^{\mathrm{T}}\right)\mathbf{x} = 2 \cdot \mathbf{x}^{\mathrm{T}}\mathbf{J}\mathbf{x} > 0 \tag{27}$$

The right-hand-side of above equation implies that matrix $\mathbf{J}$ is positive definite. In other words, $\mathbf{\Psi}(\cdot)$ is strictly monotone increasing. According to Theorem 2.3.3(a) of Pang and Facchinei (2003), it can be thus concluded that the model [VI-RUE] has one unique solution. □

Note that Condition (A), i.e., $\partial_i M_i > 0$, ensures that the ridesharing price increases as the ridesharing demand increases and the compensation decreases when the supply increases, which is exactly the requirement of the surge pricing strategies. Besides, the travel time cost and inconvenience cost are inherent costs whose values can be measured by surveys, while the ridesharing prices and compensations are artificial costs set by the TNCs based on their pricing strategies. Therefore, Condition (B) $\rho_1 > \left(\sum_{i\in RD} \frac{(\rho_i+d_i-\rho_1)^2}{4\partial_i M_i} + \sum_{i\in R} \frac{(\rho_i+d_i)^2}{4\partial_i M_i}\right)\sum_a \delta_{a,p}^w \dot{t}_a$ is actually an assumption for the employed pricing strategy for specific networks. It suggests that the term $\partial_i M_i$ should be larger than a threshold. In other words, the surge pricing strategy should not be too gentle. Moreover, apart from the predetermined coefficients and functions ρ_i and d_i, we find that the term $\sum_a \delta_{a,p}^w \dot{t}_a$ is usually very small for specific networks. For instance, if we use the Bureau of Public Roads (BPR) function, it holds that

$$\dot{t}_a = t_{a,0} be (\frac{x_a}{y_a})^{e-1} \frac{1}{y_a}, \forall a \in A \tag{28}$$

where $t_{a,0}$ denotes the free-flow travel time of link a; the parameters $b = 0.15$ and $e = 4$ in general; x_a denotes the flow on link a; y_a denotes the capacity of link a. The term $\frac{x_a}{y_a}$ is the volume-to-capacity (V/C) ratio which approximates 1. Since the capacity y_a is large, e.g., the magnitude of y_a is larger than 10^4 for all links in the Sioux-Falls network, $\dot{t}_a$ is a very small number in practice, which makes $\partial_i M_i$ have a very wide range of values under Condition (B). In summary, both Conditions (A) and (B) are mild for the pricing strategy in practice.

4. Parallel Solution Method

Most VI problems can be reformulated into complementarity problems (CPs) and then solved by commercial solvers. However, it is known that most solvers require good model formulations, gentle scales, and appropriate initial points for convergence. Take the PATH solver as an example; even though the model is well defined, a large-scale numerical experiment or an inappropriate initial point may still lead to non-convergence (Ferris and Munson, 2014). Hence, we develop an efficient solution method to find an exact solution for the large-scale RUE problems.

Because of the non-additivity of the generalized travel costs, the model [VI-RUE] involves path flows, resulting in the computationally demanding issue. The projection methods are considered very efficient to solve VI problems because of the small amount of computation time in each iteration. Since we have rigorously demonstrated the monotonicity of the model [VI-RUE], a group of projection methods for solving the monotone VI models can be utilized. In addition, to obtain an exact solution and to further speed-up the computation, we use the column generation and parallel computing techniques to design an effective solution method.

4.1 Projection methods

Before proposing the parallel solution method, we briefly introduce the projection methods. It is well-known that VI problems are identical to the following projection operator (Eaves, 1971):

$$[Q]: \mathbf{f} = P_{\Omega}[\mathbf{f} - \mathbf{\Psi}(\mathbf{f})] \tag{29}$$

where $P_{\Omega}(\cdot)$ denotes the projection of a vector $(\cdot)$ on the set Ω in the Euclidean-norm, i.e.,

$$P_{\Omega}(\cdot) = \arg\min_{\mathbf{u}\in\Omega} \|\mathbf{u} - (\cdot)\| \tag{30}$$

Among various projection methods for solving VI problems, the basic projection method proposed by Goldstein (1964) and Levitxn and Polyak (1966) is presented below:

$$[Q']: \mathbf{f}^{k+1} = P_{\Omega}[\mathbf{f}^{k} - \beta_k \mathbf{\Psi}(\mathbf{f}^{k})] \tag{31}$$

where β_k is the step size at the k-th iteration; $\mathbf{f}^k$ is the vector of the path flow at the k-th iteration. With the different conditions for convergence, many variants of the basic projection methods have been developed, including the self-adaptive projection method (He et al., 2009) and the projection-based prediction-correction method (Fu and He, 2010). Both of them require only the co-coercivity of the vector function $\mathbf{\Psi}(\cdot)$ to converge which is a milder condition than the strong monotonicity (Han and Lo, 2004).

The projection methods have a wide range of application for solving VI models of UE traffic assignment (Han et al., 2012; Jing et al., 2017; Liu et al., 2018; Meng et al., 2014). We extend the projection methods to the RUE problem. However, the projection operations in these methods usually occupy excessive computing resources, especially for large-scale problems.

A parallel-processing procedure on the projection operations is a direct and ideal engineering solution for accelerating the computation. We refer to the parallel computing method for the projection-type methods as the parallel projection (PP) method hereafter. Network decomposition is one commonly used strategy for solving the TAPs on parallel/distributed computing systems (Hribar et al., 2001; Liu and Meng, 2013). It partitions the overall network into small sub-networks. Herein, similar to the network decomposition, the

PP method decomposes the projection operation into a number of sub-projection operations. Each sub-projection operation calculates the projection for a sub-network with only one OD pair. We assign multiple processors to handle these sub-projection operations. Thus, in this PP method, each processor calculates the projection for only one sub-network each time, which significantly saves the in-memory resources, and by making full use of the processors, the computational efficiency can be significantly improved. Besides, column generation is another widely used technique to save the in-memory resources and improve the computational efficiency for the large-scale TAP problems (Galligari and Sciandrone, 2019; Ji et al., 2017). It puts new shortest paths (if any) to the path sets at each iteration, thus the computational resources for computing and storing *a priori* path sets are saved.

4.2 Parallel self-adaptive projection method incorporating column generation

Unlike the self-adaptive projection method proposed by He et al. (2009), many other projection methods need a coercive module to determine the step size β_k. Because of its mild convergence condition and no need the coercive module, we modify it and propose the following PSPM incorporating column generation to solve the model [VI-RUE].

Step 1 (Initiation): Given $\varepsilon > 0$, $\mu \in (0,1)$, $\delta \in (0,2)$, $\beta_0 > 0$, $k = 1$, $l = 0$, the initial path set P^w for each OD pair $w \in W$, and a feasible path flow vector $\mathbf{f}_w^1 \in \Omega_w$, where $\Omega_w = \{\mathbf{f}_w | \text{Eqs. (1) and (5) are satisfied}\}$.

Step 2 (Update path set): Find current shortest paths $\hat{p}_w^k$, $\forall w \in W$ with respect to link travel time $t_a(\mathbf{x}^k)$, $\forall a \in A$, and let $\hat{f}_w^k$ denote the current flow on path $\hat{p}_w^k$. Update $P^w = P^w \cup \{\hat{p}_w^k\}$ (note that $\hat{p}_w^k$ may already belong to P^w before updating) and $\mathbf{f}_w^k = \mathbf{f}_w^k \cup \{\hat{f}_w^k\}$.

Step 3 (Check stop criterion): If $\sqrt{\frac{\sum_w (\varepsilon_w^k)^2}{\sum_w (\sigma_w^k)^2}} < \varepsilon$, then stop; otherwise, go to Step 4. Here we have:

$$[Q_w]: \mathbf{g}_w^k := P_{\Omega_w}[\mathbf{f}_w^k - \mathbf{\Psi}(\mathbf{f}_w^k)] \tag{32}$$

$$\varepsilon_w^k := \left\| \mathbf{f}_w^k - \mathbf{g}_w^k \right\| \tag{33}$$

$$\sigma_w^k \coloneqq \left\|\mathbf{f}_w^k\right\| \tag{34}$$

Step 4. (Determine step size) Let

$$\beta_k \coloneqq \mu^l \beta_{k-1} \tag{35}$$

$$[Q_w']: \mathbf{f}_w^{k+1} \coloneqq P_{\Omega_w}[\mathbf{f}_w^k - \beta_k \mathbf{\Psi}(\mathbf{f}_w^k)] \tag{36}$$

$$\alpha_w^k \coloneqq \beta_k ||\mathbf{\Psi}\left(\mathbf{f}_w^k\right) - \mathbf{\Psi}(\mathbf{f}_w^{k+1})||^2 \tag{37}$$

$$\omega_w^k \coloneqq (\mathbf{f}_w^k - \mathbf{f}_w^{k+1})^{\mathrm{T}}\left[\mathbf{\Psi}\left(\mathbf{f}_w^k\right) - \mathbf{\Psi}\left(\mathbf{f}_w^{k+1}\right)\right] \tag{38}$$

If $\frac{\sum_w \alpha_w^k}{\sum_w \omega_w^k} \leq 2 - \delta$, let $k = k + 1$ and go to Step 2; otherwise, $l = l + 1$, repeat Step 4.

The projection operations in $[Q_w]$ and $[Q_w']$ shown in Steps 3 and 4 are solved by the following quadratic programming:

$$\arg\min_{\mathbf{h}\in\Omega_w} ||\mathbf{h} - [\mathbf{f}_w^k - \beta_k \mathbf{\Psi}\left(\mathbf{f}_w^k\right)]|| \tag{39}$$

where $\beta_k = 1$ for $[Q_w]$. Step 2 is known as the column generation that augments the path set P^w by including the path $\hat{p}_w^k$ that is the shortest in terms of travel time at each iteration k. Leventhal et al. (1973) proved that column generation guarantees a global convergence without listing all the paths to save the in-memory resources and improve the computational efficiency. It is widely used for the traditional UE problem where the travel time is taken into account to find the shortest path. Although it is the generalized travel cost rather than the travel time that affects travelers' route choice in the RUE problem, according to Proposition 4, we know that the shortest paths in terms of travel time between an OD pair are also the shortest paths in terms of generalized travel cost for all roles between the OD pair for the proposed model [VI-RUE]. Thus, we only need to find the shortest paths in terms of travel time, and the column generation can be easily incorporated into the solution method. For other RUE models where Proposition 4 does not hold, the incorporation of column generation may be non-trivial. In this way, the benefits of saving in-memory resources and improving computational efficiency partially result from our model development. Moreover, since the column generation and parallel computing techniques do not change the convergence condition for the self-adaptive projection method, the convergence of the proposed method follows He et al. (2009).

4.3 Performance measures

As the size of the path set increases, the execution time and the in-memory requirements may increase nonlinearly, where the former one measures the computational efficiency and the latter one affects the computational feasibility. If a computing implementation takes excessive time to execute, the computational efficiency is low; if it requires more in-memory resources than provided, the computing may be infeasible. Thus, the execution time and the in-memory requirement will be used as the performance measures in the evaluation of the proposed parallel method against the traditional projection method.

Besides, several other performance measures are used to evaluate the performance of parallel computing implementations in the literature, among which the most frequently used one is the *speedup* that measures the computation efficiency of parallel computing approaches (Liu and Meng, 2013). The speedup for *j* processors can be defined as:

$$S(j) = \frac{T_1}{T_j} \tag{40}$$

where T_j is the execution time when *j* processors are involved in the calculation. Note that as the number of processors increases, the computing time spent in data communication would keep increasing. Therefore, the speedup would be a sub-linear function with respect to the number of processors.

Another performance measure is called the time-saving ratio proposed by Zhang et al. (2017). It measures the ratio of the execution time saved by the parallel method and is defined as:

$$T(j) = \frac{T_0 - T_j}{T_0} \tag{41}$$

where T_0 denotes the execution time of the traditional (non-parallel) method.

5. Numerical Experiments

In this section, three networks, i.e., Braess network, Sioux-Falls network, and Eastern-Massachusetts network, will be used for the numerical experiments. We first use the Braess network to analyze the impact of ridesharing services on the network and carry out the sensitivity analysis on the VOTs, inconvenience coefficients, pricing coefficients, benchmark prices, and trip costs to provide some practical insights. We then use the Sioux-Falls network and the Eastern-Massachusetts network to examine the computational feasibility and efficiency of the proposed solution method. The results are obtained by solving the VI model using the developed PSPM.

5.1 Braess network

We first examine how the introduction of ridesharing affects the equilibrium flow pattern and the resultant travel costs of all the roles by comparing the UE state with and without ridesharing services. The Braess network, its link cost functions and travel demand are shown in Fig. 1. There are three paths in total: Path 1: 1-2-4, Path 2: 1-3-4 and Path 3: 1-2-3-4.

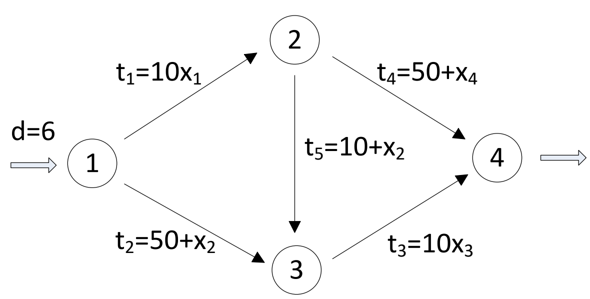

Fig. 1. Braess network.

We assume that there are five roles and the functions $I_i(\cdot)$ and $M_i(\cdot)$ for the inconvenience costs, the prices, and the compensations follow the affine function. The generalized travel cost functions of the five roles are expressed by

$$\begin{cases} C_{p,1}^{w} = \rho_1 t_p^w + c_t \\ C_{p,2}^{w} = \rho_2 t_p^w + \gamma_2 t_p^w - \left(B_2^w - m_2 \sum_p f_{p,2}^w\right) + c_t \\ C_{p,3}^{w} = \rho_3 t_p^w + \gamma_3 t_p^w - \left(B_3^w - m_3 \sum_p f_{p,3}^w\right) + c_t\,, \forall w, p \\ C_{p,4}^{w} = \rho_4 t_p^w + \gamma_4 t_p^w + \left(B_4^w + m_4 \sum_p f_{p,4}^w\right) \\ C_{p,5}^{w} = \rho_5 t_p^w + \gamma_5 t_p^w + \left(B_5^w + m_5 \sum_p f_{p,5}^w\right) \end{cases} \tag{42}$$

where γ_i is the inconvenience coefficient for role i; and m_i is the coefficient for calculating the surge price or compensation for role i. For simplicity, we assume that the riders' VOT is lower than their drivers', i.e., $\rho_{\mathcal{T}_r(i)} < \rho_i, \forall i \in \{2,3\}$. Besides, since the inconvenience costs are relative to the numbers of in-vehicle strangers, we also assume that the inconvenience coefficient for the 2-rider ridesharing is higher than that of 1-rider, i.e., $\gamma_3 = \gamma_5 > \gamma_2 = \gamma_4$. We assume $m_i > 0$ to meet the requirement of surge pricing strategy. The values of these parameters are listed in Table 1.

Table 1. Parameter setting for the Braess network

Description	Constants	Values
Values of time	ρ_1, ρ_2, ρ_3, ρ_4, ρ_5	1, 0.8, 0.8, 0.4, 0.4
Inconvenience coefficients	γ_2, γ_3, γ_4, γ_5	0.3, 0.4, 0.3, 0.4
Pricing coefficients	m_2, m_3, m_4, m_5	5, 5, 1, 1
Benchmark price	B_i	20
Trip cost	c_t	1

Table 2 shows the values of the concerned variables at the RUE state. Specifically, it can be seen that the generalized travel cost $\tilde{C}_{p,i}$ of each role i on the used path p is minimal, which aligns with the RUE principle. The travel time t_p on the used path is minimal as Proposition 3 exhibits. In addition, we find that ridesharing participants only exist on Path 3. For the Braess network without ridesharing services, the travel time is 92. However, with ridesharing, the travel time on Paths 1 and 2 reduces to 82.4, even though no ridesharing participants travel on them. This is because some travelers spontaneously switch to riders due to the introduction of ridesharing, which reduces the number of vehicle trips. Therefore, ridesharing reduces the travel time for not only ridesharing participants but also solo drivers. All the involved players benefit from ridesharing services. This finding provides strong justification to promote ridesharing services for the sake of congestion mitigation.

Table 2. Numerical results for the Braess network

(p,i)	With ridesharing			Without ridesharing	
	$\tilde{C}_{p,i}$	$f_{p,i}$	t_p	f_p	t_p
(1,1)	83.4	0			
(1,2)	85.4	0			
(1,3)	79.9	0	82.4	2	92
(1,4)	80.4	0			
(1,5)	85.9	0			
(2,1)	83.4	0			
(2,2)	85.4	0			
(2,3)	79.9	0	82.4	2	92
(2,4)	80.4	0			
(2,5)	85.9	0			
(3,1)	79.0	0.475			
(3,2)	80.6	2.762			
(3,3)	74.6	0	78.0	2	92
(3,4)	77.4	2.762			
(3,5)	82.4	0			

We further investigate the impacts of the VOTs, the inconvenience coefficients, and the pricing coefficients on the role choice of the travelers. Moreover, since the prices and trip costs may directly affect the supply and demand and then the number of vehicle trips, we also examine the impact of the benchmark prices and trip costs on the role choice, the vehicle trips and the travel time.

Without loss of generality, we take the VOT of riders and the inconvenience coefficient for 2-rider ridesharing as examples. Figure 2 shows the variation of the role choice against the VOT of riders. It can be seen that the number of riders decreases, while the number of ridesharing drivers first increases then decreases since restricted by the number of riders. As the VOT of riders increases, the riders switch to other players, i.e., the ridesharing drivers and solo drivers. It suggests that VOT is an influential factor for the travelers' role choice. If the riders have a higher VOT, they will perceive higher travel time costs, and the difference between the travel time costs of riders and those of drivers will be narrowed. As a result, more riders will switch to drivers. Figure 3 shows the variation of the two ridesharing driver roles. We omit the riders because the riders $\mathcal{T}_r(i)$ are exactly N_i times as many as the ridesharing drivers $i, \forall i \in RD$. It can be seen that, as the inconvenience coefficient increases, the number of 2-rider ridesharing activities decreases; and that of 1-rider ridesharing activities increases. This is because, as 2-rider ridesharing activities become more inconvenient, fewer ridesharing participants would like to participate in them. They change from 2-rider ridesharing to 1-rider that is more attractive. It decreases the occupancy ratio of ridesharing vehicles. This finding suggests that the inconvenience cost may be a vital factor for the participants' choice of ridesharing services. The TNCs can promote their premium ridesharing services that have fewer in-vehicle riders, e.g., the UberX, KuaiChe, and GrabCar services, by improving the service quality and reducing the inconvenience cost.

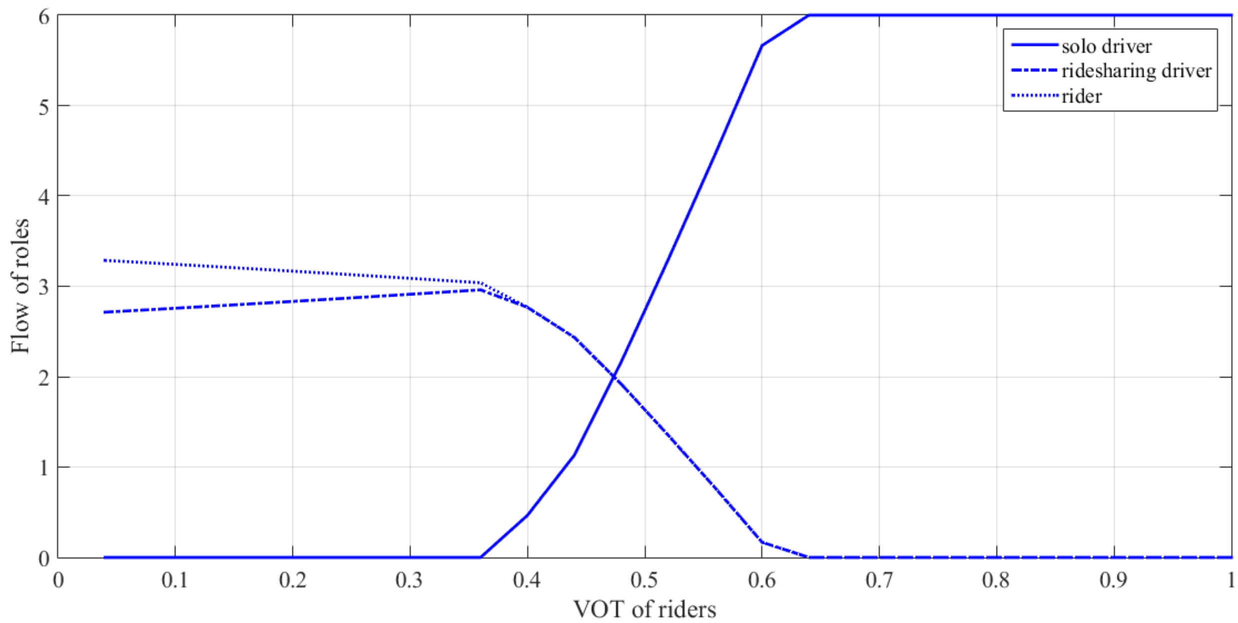

Fig. 2. The effect of the VOT of riders on the role choice

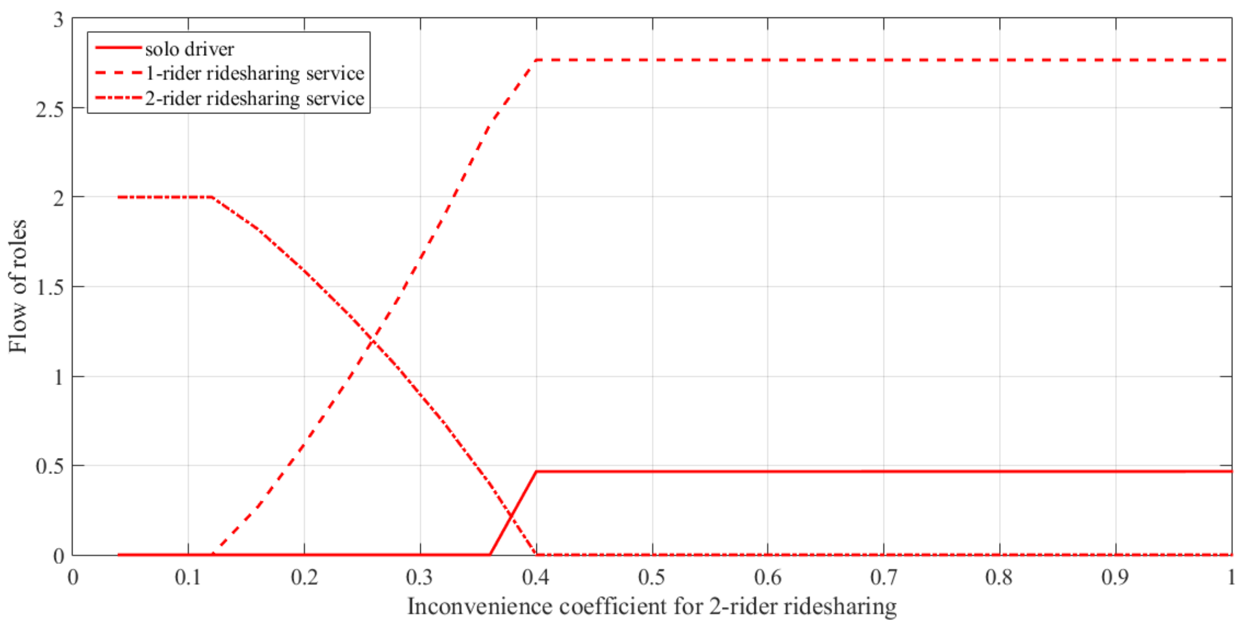

Fig. 3. The effect of the inconvenience coefficient for 2-rider ridesharing on the role choice.

The increasing VOTs and inconvenience coefficients may also influence the average occupancy ratio of the whole network and the market penetration rate of ridesharing services that are concerned by the traffic managers and the TNCs, respectively. We define the average occupancy ratio as the ratio of all the travelers to all the drivers, i.e., $\frac{q^w}{\sum_{i\in SD\cup RD}\sum_p f_{p,i}^w}$, and the market penetration rate as the ratio of ridesharing participants to all the travelers, i.e., $\frac{\sum_{i\in RD\cup R}\sum_p f_{p,i}^w}{q^w}$. Figure 4 shows how the variation of the VOTs and the inconvenience coefficients affects the average occupancy ratio and the market penetration rate. As the VOTs and inconvenience coefficients increase, the average occupancy ratio and the market penetration rate decrease simultaneously. This observation suggests that a low travel time cost or inconvenience cost of each ridesharing participant may help increase the average occupancy ratio and the market penetration rate. Traffic managers and TNCs may try to reduce the travel time cost and the inconvenience cost for ridesharing participants to mitigate traffic congestion and attract customers.

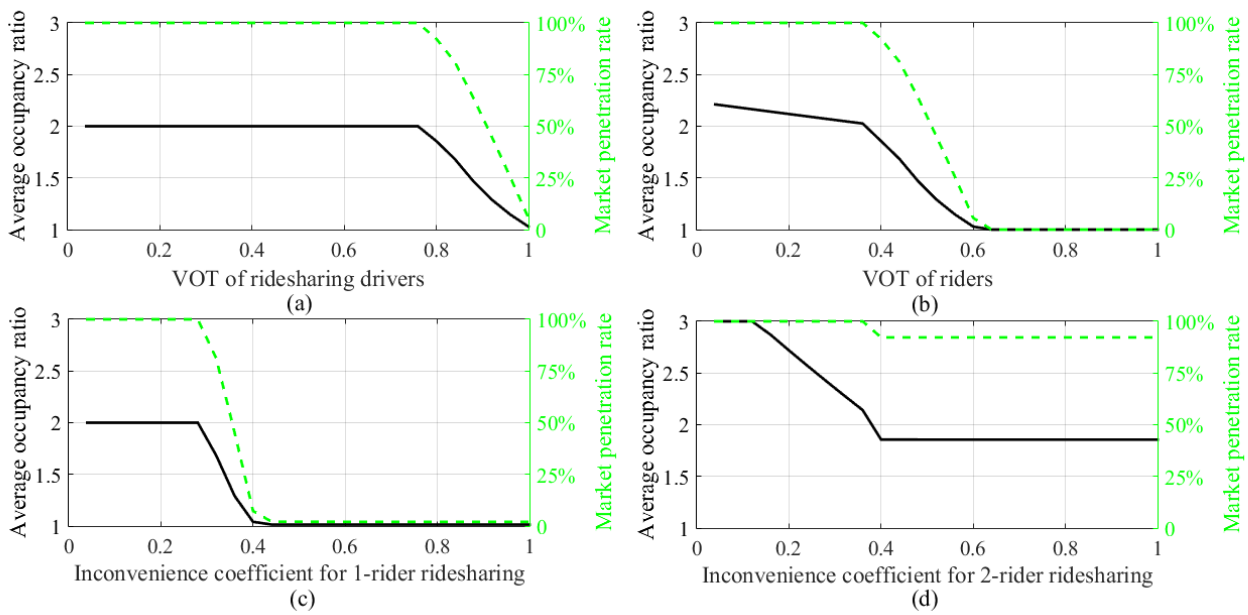

Fig. 4. The effect of the VOTs and inconvenience coefficients on the average occupancy ratio and market penetration rate.

Figure 5 shows the variation of the role choice against the pricing coefficients. It can be seen that, as the pricing coefficient increases, the number of ridesharing participants decreases; and that of solo drivers increases. This is because, as ridesharing activities become more expensive for riders or less profitable for ridesharing drivers, their generalized travel costs become higher, which reduces travelers' willingness to participate in ridesharing. This finding suggests that although an overly surged pricing strategy increases TNC's profit per ridesharing activity, it will also decrease the number of ridesharing activities. A proper pricing strategy may help TNCs maximize their profit.

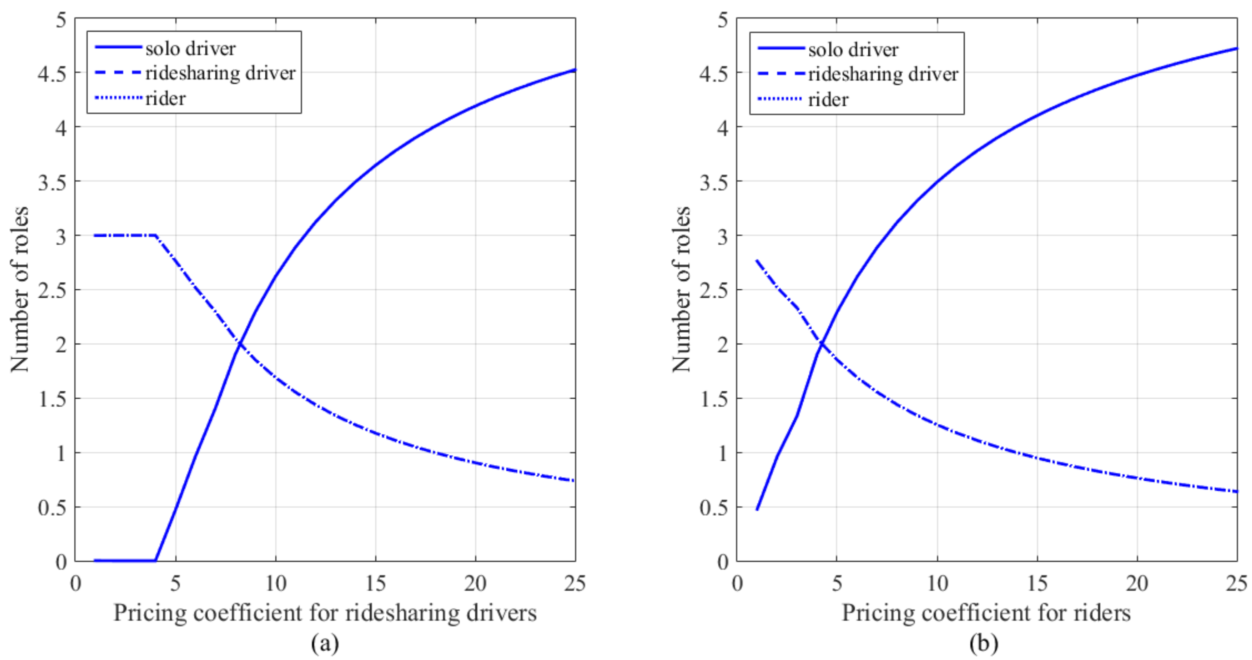

Fig. 5. The effects of the pricing coefficients on the role choice.

Figure 6 shows the variation of the role choice against the benchmark price and trip costs. As the benchmark price increases, the number of riders decreases and that of ridesharing drivers increases, which shows that a high price may restrain the ridesharing demand and stimulate the supply. Moreover, we observe that the number of 1-rider ridesharing activities increases and that of 2-rider ridesharing activities decreases. This suggests that a high price may draw the ridesharing participants into the ridesharing services with fewer in-vehicle riders. When the trip costs increase, more travelers want to take a ride rather than to drive, which makes the 2-rider ridesharing service more attractive.

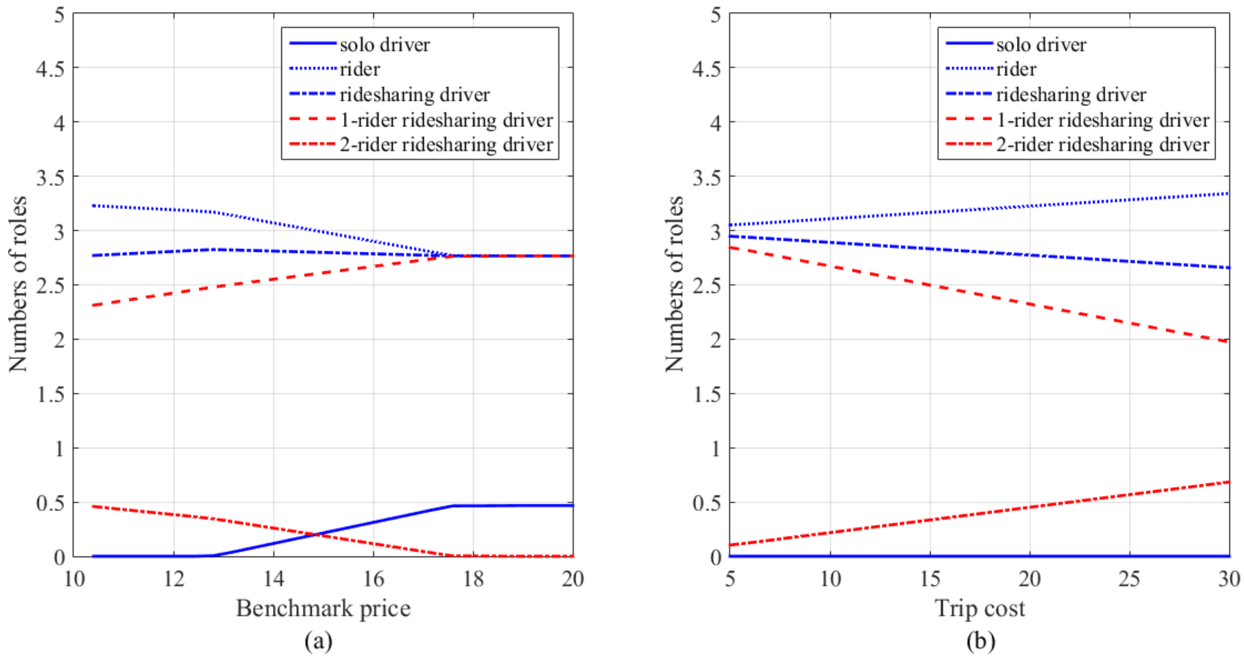

Fig. 6. The effects of the benchmark price and trip cost on the role choice.

Figure 7 shows the variation of the number of vehicle trips and the travel time against the benchmark price and trip costs. It suggests that a low benchmark price (or a high trip cost) may increase the number of riders and reduce the vehicle trips and thus the travel time of each traveler. We investigate the relationship between the travel time and the number of riders by sampling in Figure 8, where each marker represents a sample. It suggests that the more the riders (i.e., the more vehicle trips reduced by ridesharing), the lower the travel time. Note that this is only a general speaking since the well-known Braess paradox may happen when the number of vehicle trips changes. An interesting discussion about the relationship between the Braess paradox and the amount of traffic demand [vehicle trips] can be seen in Ma et al. (2018b).

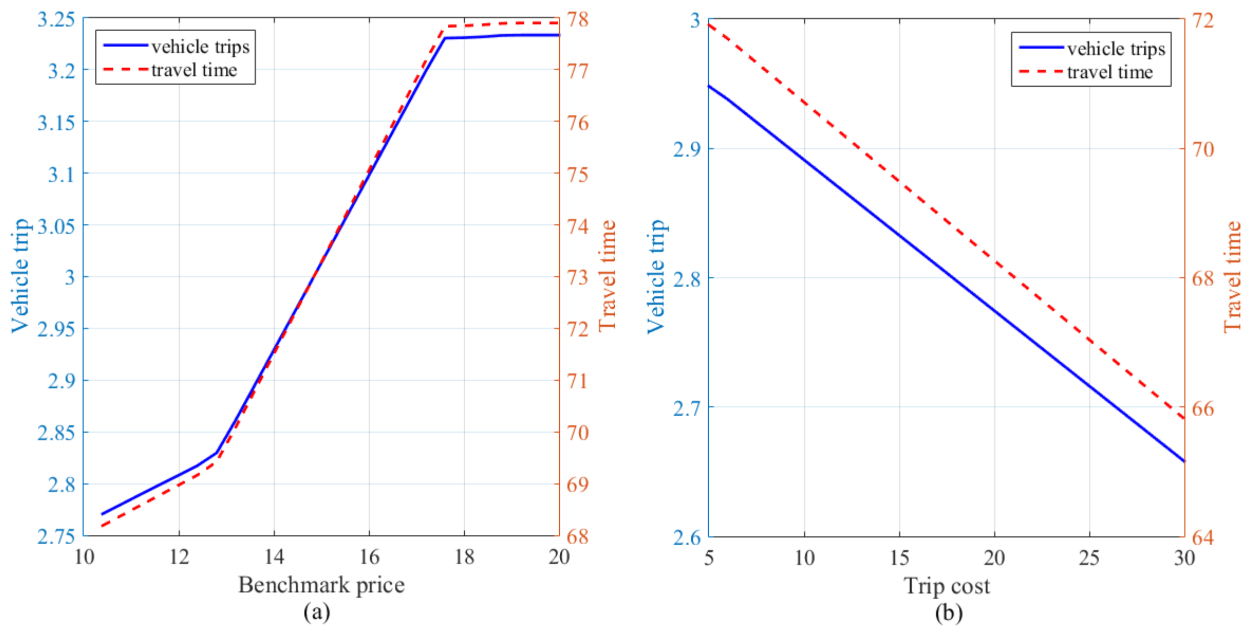

Fig. 7. The effect of the benchmark price and trip cost on travel time and vehicle trips.

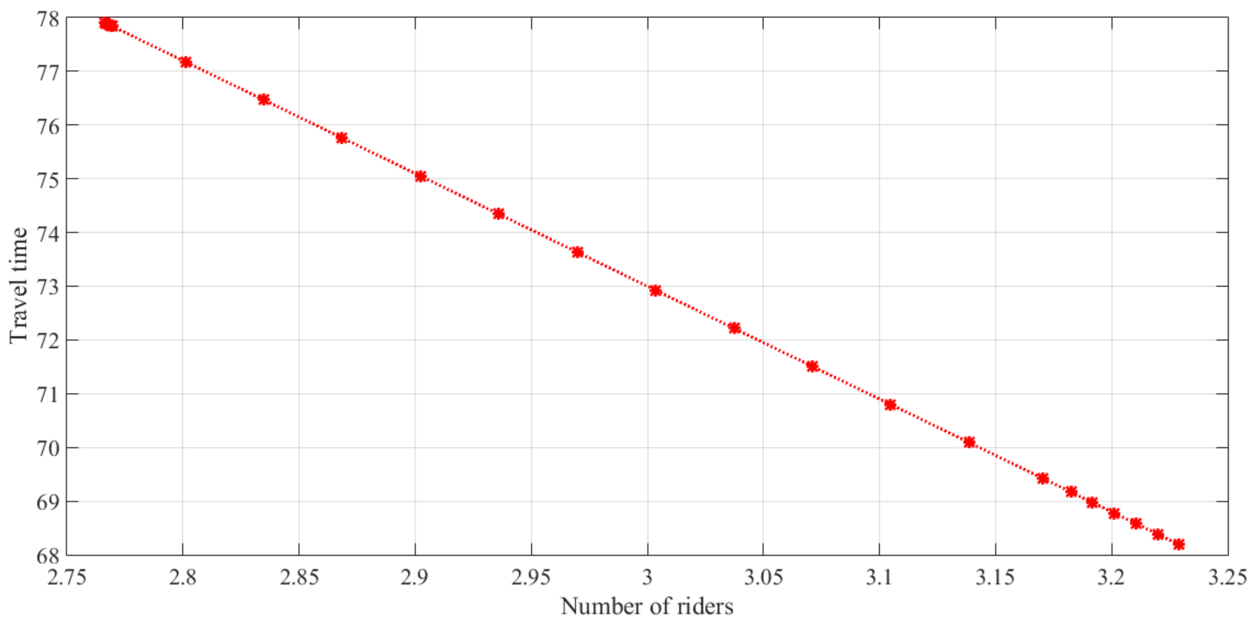

Fig. 8. The effect of the number of riders on travel time.

5.2 Sioux-Falls network

Herein, we solve the RUE problem for the Sioux-Falls network to assess the validity of the proposed solution method. The link flows and the number of paths between each OD pair at the RUE state are illustrated. The computational feasibility and efficiency of the proposed solution method are tested by comparing the in-memory requirement and the execution time of the traditional method and the proposed method when only one processor is utilized. Finally, to test the performance in parallel computing of the proposed method, the variation of the speedup and the time-saving ratio against the number of utilized processors will be investigated. We use the well-known Sioux-Falls network for the test, which has 24 nodes, 76 links, and 528 OD pairs. The topology of the Sioux-Falls network is shown in Figure 9. The Bureau of Public Roads (BPR) function is used to describe the link travel time:

$$t_a(x_a) = t_{a,0}\left[1 + b\left(\frac{x_a}{y_a}\right)^e\right], \forall a \in A \tag{43}$$

where $t_{a,0}$ denotes the free-flow travel time of link a; y_a denotes the capacity of link a; and the parameters $b = 0.15$, $e = 4$ in general. The values of the free-flow travel time, the link capacity, and the OD trips can be found in Bar-Gera (2016).

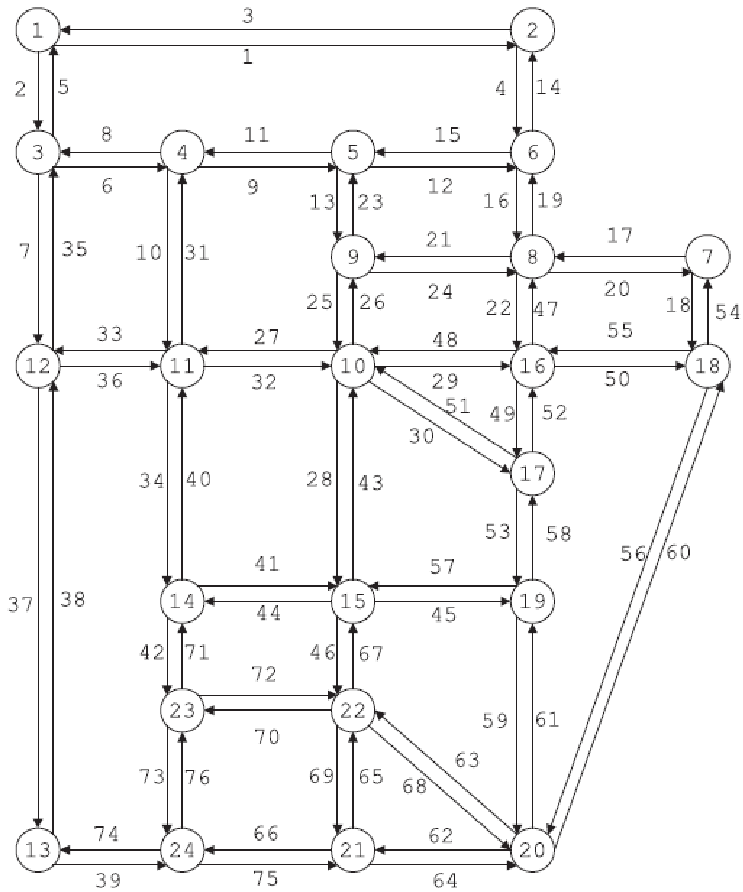

Fig. 9. Sioux-Falls network.

The computing platform used for this study is a PC system using Intel Core i7 3770 (Quad-Core; Intel® Core™, Santa Clara, CA, USA) processor, with a clock speed of 3.40 GHz, 1 MB L2 cache per core, 8 MB L3 cache, and 6 GB of 1333 MHz DDR3 RAM. The operating system is Windows 7 Enterprise SP1 64 Bit version. The programs for this study are coded in MATLAB R2015a.

We solve the RUE problem by using the proposed solution method incorporating column generation. Table 3 illustrates the link flows at the RUE state. Besides, it is known that the column generation augments the initial path set by including new shortest paths (if any) at each iteration to ensure a globally optimal solution (Leventhal et al., 1973). Thus, the path set increases as the solution method proceeds, which makes the computational performance strongly depends on the size of the path set. However, it has been supported by many studies that, although the actual number of paths in the network may be large, the number of paths included in the working path set P^w remains small (Leventhal et al., 1973). To verify this, we show the number of paths at the RUE state. Table 4 suggests that the number of paths in each path set is not more than 5. Details can be seen in Appendix B.

Table 3. Link flows at the RUE state

Link	Flow	Link	Flow	Link	Flow	Link	Flow
1	4796.3	20	12559.1	39	10948.3	58	10101.8
2	8325.5	21	6963.4	40	9609.7	59	8609.3
3	4808.0	22	8237.6	41	8936	60	18837.9
4	5607.2	23	15499.5	42	8248.7	61	8631
5	8313.0	24	7022.8	43	22537.8	62	6456.7
6	14073.8	25	21793.8	44	8929.6	63	6910.7
7	10043.0	26	21938.3	45	18221.7	64	6497.1
8	14082.4	27	17512.1	46	18123.6	65	8383.2
9	18323.7	28	22015.8	47	8364.1	66	10175.8
10	5477.2	29	11087.1	48	11044.6	67	18130.2
11	18408.3	30	7399.9	49	11417.8	68	6910.5
12	8632.4	31	5398.0	50	15219.3	69	8393.1
13	15409.7	32	17586.1	51	8002.2	70	9508.9
14	5618.9	33	8250.1	52	11420.3	71	8245.5
15	8625.7	34	9853.8	53	10099.5	72	9525.2
16	12641.6	35	10021.8	54	15395.5	73	7750.5
17	12541.7	36	8272.1	55	15222.4	74	10906.9
18	14720.3	37	12725.0	56	18819.2	75	10204.8
19	12645.1	38	12724.5	57	18241.0	76	7763.1

Table 4. Number of paths at the RUE state

# of paths in the overall network	# of paths between OD pair	# of OD pairs
1090	1	169
	2	203
	3	120
	4	25
	5	11
	≥ 6	0

Besides the column generation, many other path generation algorithms can be used to generate the path sets for the proposed solution method. For example, the k-shortest path algorithm proposed by Yen (1971) can generate path sets that contain desired numbers of paths. Next, to investigate the variation of the performance of the proposed method against the size of the path set, we use the k-shortest path algorithm instead of the column generation to enumerate fixed path sets P^w for illustration. The projection operations of projection-type methods take up most of the computational resources, thus we focus on the projection operations to investigate the computational feasibility and efficiency of the proposed method. Since the proposed method decomposes the original projection operation $[Q]$ into 528 sub-projection operations $[Q_w]$s, to make it fair, we compare the execution times of the traditional method and the proposed method to solve one $[Q]$ and 528 $[Q_w]$s, respectively. Besides, only one core of the processor is opened for the proposed method, thus the merit of parallel computing is excluded. Figure 10 and Figure 11 show the variation of the in-memory requirement and the execution time, respectively, of the projection operations of both methods against the number of paths. It can be seen that, if we generate more than 4 paths for each OD pair, the traditional method fails because more in-memory is needed than provided, while the proposed method still performs well, which suggests that the proposed method has a better computational feasibility. Moreover, as the number of paths increases, both the in-memory requirement and the execution time of the traditional method increase sharply, while those of the proposed method rise slowly. It suggests that the proposed method is less sensitive to the size of the path set.

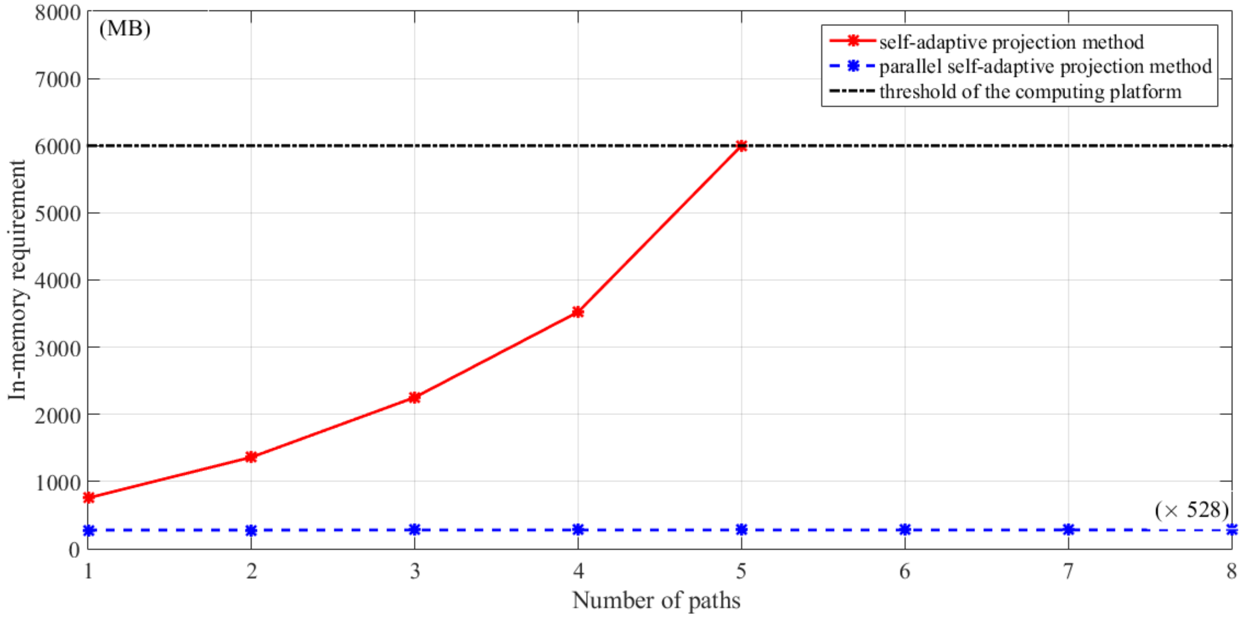

Fig. 10. The variation of the in-memory requirement against the number of paths per OD pair

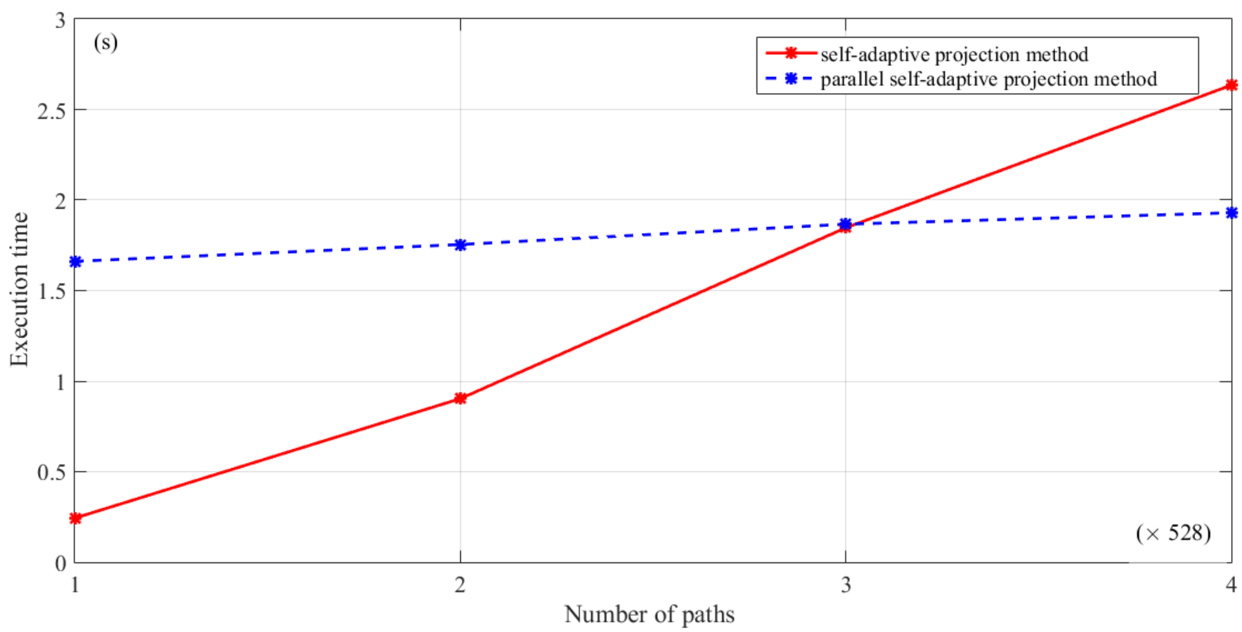

Fig. 11. The variation of the execution time against the number of paths per OD pair

Next, we use more cores of the processor to numerically test the performance of parallel computing of the proposed method. Table 5 shows the variation of the execution time, the speedup, and the time-saving ratio against the number of utilized cores when the number of paths is 4×528 and the accuracy level is $\varepsilon = 10^{-3}$. Compared with T_1, the execution time is inherently reduced when multiple cores are used. Moreover, as the number of cores increases, the speedup and the time-saving ratio keep increasing. These observations suggest the validity of the proposed parallel method and imply that this method has sound parallelism, i.e., the time elapsed in data communication is less than the time saved by parallel computing, and the overall idle time is trivial.

Table 5. Test of the parallel solution method in the Sioux-Falls network (4×528 paths, $\varepsilon = 10^{-3}$)

Non-parallel execution time (s) T_0	No. of cores j	Execution time (s) T_j	Speedup $S(j)$	Time-saving ratio $T(j)$
7994.9	1	6834.7	1.000	0.145
	2	3945.5	1.732	0.506
	3	3099.4	2.205	0.612
	4	2753.3	2.482	0.656

5.3 Eastern-Massachusetts network

Herein, we use another large-scale network to further demonstrate the effectiveness of the proposed solution method to solve realistically-sized problems. For large-scale networks, finding the shortest paths (i.e., column generation) may occupy excessive computing resources. We hence test the parallel solution method incorporating column generation in the Eastern-Massachusetts (EMA) network which has 258 links and 74 nodes. The topology, the parameters for the BPR function, and the OD trips of the EMA network can be found in Bar-Gera (2016). To check the performance of the solution method under different levels of congestion, we expand the OD trips by up to four times. Similar to the traditional UE problems, the levels of congestion also affect the convergence as shown in Table 6. For an extremely congested network (with 4 times of the OD trips), the proposed solution method can still converge in an acceptable computational time.

Table 6. Test of the parallel solution method in the EMA network (4 cores, column generation, $\varepsilon = 10^{-3}$)

OD trips	Execution time (h)
1x	0.25
2x	1.01
3x	4.56
4x	11.97

6. Conclusions

This study develops a VI model for the RUE problem under the OD-based surge pricing strategy. It takes the first attempt to introduce an OD-based path-independent surge pricing strategy into the RUE problem. The developed VI model explicitly takes into account how to formulate a more realistic cost function that captures the non-additive generalized travel costs of ridesharing travelers. Compared with existing studies of the RUE problem, the proposed model formulates the capacity in carrying riders more explicitly, which removes the assumptions required by existing techniques and widens the application of existing RUE models. We propose the PSPM incorporating column generation that can be applied on the parallel/distributed computing systems to solve the large-scale problems and to speed up the computation. Finally, numerical experiments are conducted to provide some practical insights and to assess the computational feasibility and efficiency of the proposed solution method. In short, the contributions of this study are fourfold: (i) we consider an OD-based path-independent surge pricing strategy and an explicit assignment of riders; (ii) an interesting VI formulation for the RUE problem is developed; (iii) a practical solution method based on the column generation and parallel computing techniques is proposed; and (iv) numerical experiments are conducted to provide some insights and demonstrate the effectiveness of the proposed method.

Future challenges may include: (i) the consideration on the elastic demand, the link capacity constraints, and the uncertainty; (ii) more travel modes for travelers to choose; and (iii) the extension to the so-called dedicated ridesharing which allows dedicated drivers to participate in.

Acknowledgments

We are grateful to the two anonymous reviewers for their valuable comments and suggestion made to the early versions of this manuscript. This research is supported by the research project “Congestion Management Policies for Road Networks with Ridesharing Services” funded by Singapore Ministry of Education Academic Research Fund Tier 2 (MOE2017-T2-2-128). The first and fourth authors would like to thank the support from the National Natural Science Foundation of China (No. 51178110 and No. 51378119), the Scientific Research Foundation of the Graduate School of Southeast University (No. YBJJ184), and the China Scholarship Council (CSC).

References

Amey, A.M., 2010. Real-Time Ridesharing: Exploring the Opportunities and Challenges of Designing a Technology-based Rideshare Trial for MIT Community. Massachusetts Institute of Technology, MA, USA.

Armijo, L., 1966. Minimization of functions having Lipschitz continuous first partial derivatives. Pacific Journal of Mathematics 16, 1–3.

Ban, X. (Jeff), Pang, J.S., Liu, H.X., Ma, R., 2012. Modeling and solving continuous-time instantaneous dynamic user equilibria: A differential complementarity systems approach. Transportation Research Part B: Methodological 46, 389–408. https://doi.org/10.1016/j.trb.2011.11.002

Bar-Gera, H., 2016. Transportation Networks for Research [WWW Document]. URL https://github.com/bstabler/TransportationNetworks

Beckmann, M.J.., Golob, T.F., 1974. Traveler decision and traffic flows: a behavioral theory of network equilibrium, in: Buckley, D.J. (Ed.), Proceedings of the 5th International Symposium on the Theory of Traffic Flow and Transportation. Elsevier, Sydney, pp. 453–482.

Campbell, H., 2018. The Rideshare Guide: Everything You Need to Know about Driving for Uber, Lyft, and Other Ridesharing Companies. Skyhorse Publishing.

Catriona, H.-J. (cosmopolitan), 2016. This girl was charged over £100 by an Uber driver who took her on a detour to “avoid traffic” [WWW Document]. URL https://www.cosmopolitan.com/uk/reports/news/a42218/girl-charged-extra-uber-driver-detour-traffic/

Chan, N.D., Shaheen, S.A., 2012. Ridesharing in North America: past, present, and future. Transport Reviews 32, 93–112. https://doi.org/10.1080/01441647.2011.621557

Chen, A., Zhou, Z., Lam, W.H.K., 2011. Modeling stochastic perception error in the mean-excess traffic equilibrium model q. Transportation Research Part B 45, 1619–1640. https://doi.org/10.1016/j.trb.2011.05.028

Daganzo, C.F., 1981. Equilibrium model for carpools on an urban network. Transportation Research Record: Journal of the Transportation Research Board 835.

Di Lorenzo, D., Galligari, A., Sciandrone, M., 2014. A convergent and efficient decomposition method for the traffic assignment problem. Computational Optimization and Applications 60, 151–170. https://doi.org/10.1007/s10589-014-9668-6

Di, X., Liu, H.X., Ban, X. (Jeff), Yang, H., 2017. Ridesharing user equilibrium and its implications for high-cccupancy toll lane pricing. Transportation Research Record: Journal of the Transportation Research Board 2667, 39–50. https://doi.org/10.3141/2667-05

Di, X., Ma, R., Liu, H.X., Ban, X. (Jeff), 2018. A link-node reformulation of ridesharing user equilibrium with network design. Transportation Research Part B: Methodological 112, 230–255. https://doi.org/10.1016/j.trb.2018.04.006

Dial, R.B., 1997. Bicriterion traffic assignment: efficient algorithms plus examples. Transportation Research Part B: Methodological 31, 357–379.

Eaves, B.C., 1971. On the basic theorem of complementarity. Mathematical Programming 1, 68–75.

Ferris, M.C., Munson, T.S., 2014. Path 4.7, Gams Corporation. Washington.

Ferris, M.C., Pang, J.S., 1997. Engineering and economic applications of complementarity problems. SIAM Review 39, 669–713.

Fu, X., He, B., 2010. Self-adaptive projection-based prediction-correction method for constrained variational inequalities. Frontiers of Mathematics in China 5, 3–21. https://doi.org/10.1007/s11464-009-0045-1

Furuhata, M., Dessouky, M., Ordóñez, F., Brunet, M.E., Wang, X., Koenig, S., 2013. Ridesharing: the state-of-the-art and future directions. Transportation Research Part B: Methodological 57, 28–46. https://doi.org/10.1016/j.trb.2013.08.012

Galligari, A., Sciandrone, M., 2019. A computational study of path-based methods for optimal traffic assignment with both inelastic and elastic demand. Computers and Operations Research 103, 158–166. https://doi.org/10.1016/j.cor.2018.11.004

Goldstein, B.Y.A.A., 1964. Convex programming in hilbert space. Bulletin of the American Mathematical Society 70, 709–710.

Grab, 2018. Why should you use GrabCar? [WWW Document]. URL https://www.grab.com/my/car/

Hall, J., Kendrick, C., Nosko, C., 2015. The effects of Uber's surge pricing : a case study request a ride, Working Paper.

Han, D., Lo, H.K., 2004. Solving non-additive traffic assignment problems: A descent method for co-coercive variational inequalities. European Journal of Operational Research 159, 529–544. https://doi.org/10.1016/S0377-2217(03)00423-5

Han, D., Zhang, H., Qian, G., Xu, L., 2012. An improved two-step method for solving generalized Nash equilibrium problems. European Journal of Operational Research 216, 613–623. https://doi.org/10.1016/j.ejor.2011.08.008

Han, K., Friesz, T.L., Szeto, W.Y., Liu, H., 2015. Elastic demand dynamic network user equilibrium : Formulation, existence and computation 81, 183–209. https://doi.org/10.1016/j.trb.2015.07.008

He, B., He, X., Liu, H.X., Wu, T., 2009. Self-adaptive projection method for co-coercive variational inequalities. European Journal of Operational Research 196, 43–48. https://doi.org/10.1016/j.ejor.2008.03.004

Hribar, M.R., Taylor, V.E., Boyce, D.E., 2001. Implementing parallel shortest path for parallel transportation applications. Parallel Computing 27, 1537–1568.

Ji, X., Ban, X. (Jeff), Li, M., Zhang, J., Ran, B., 2017. Non-expected route choice model under risk on stochastic traffic networks. Networks and Spatial Economics 17, 777–807. https://doi.org/10.1007/s11067-017-9344-3

Jing, W., Kim, I., Ramezani, M., Liu, Z., 2017. Stochastic traffic assignment of mixed electric vehicle and gasoline vehicle flow with path distance constraints. Transportation Research Procedia 21, 65–78. https://doi.org/10.1016/j.trpro.2017.03.078

Johnson, C.R., 1970. Positive definite matrices. The American Mathematical Monthly 77, 259–264.

Leventhal, T., Nemhauser, G., Trotter, L., 1973. A column generation algorithm for optimal traffic assignment. Transportation Science 7, 168–176. https://doi.org/10.1287/trsc.7.2.168

Levitxn, E.B. and Polyak, B.T., 1966. Constrained minimization methods. USSR Computational Mathematics and Mathematical Physics 6, 1–50.

Liu, Y., Li, Y., 2017. Pricing scheme design of ridesharing program in morning commute problem. Transportation Research Part C: Emerging Technologies 79, 156–177. https://doi.org/10.1016/j.trc.2017.02.020

Liu, Z., Chen, X., Meng, Q., Kim, I., 2018. Remote park-and-ride network equilibrium model and its applications. Transportation Research Part B: Methodological 117, 37–62. https://doi.org/10.1016/j.trb.2018.08.004

Liu, Z., Meng, Q., 2013. Distributed computing approaches for large-scale probit-based stochastic user equilibrium problems. Journal of Advanced Transportation 47, 553–571. https://doi.org/10.1002/atr.177

Long J., Tan W., Szeto W.Y., Li Y., 2018. Ride-sharing with travel time uncertainty. Transportation Research Part B: Methodological 118, 143–171.

Ma, J., Cheng, L., Li, D., 2018a. Road maintenance optimization model based on dynamic programming in urban traffic network. Journal of Advanced Transportation 2018, 1–11. https://doi.org/10.1155/2018/4539324

Ma, J., Li, D., Cheng, L., Lou, X., Sun, C., Tang, W., 2018b. Link restriction: methods of testing and avoiding Braess paradox in networks considering traffic demands. Journal of Transportation Engineering, Part A: Systems 144, 1–11. https://doi.org/10.1061/JTEPBS.0000111.

Ma, R., Zhang, H.M., 2017. The morning commute problem with ridesharing and dynamic parking charges.

Transportation Research Part B: Methodological 106, 345–374. https://doi.org/10.1016/j.trb.2017.07.002

Masoud, N., Jayakrishnan, R., 2017. A real-time algorithm to solve the peer-to-peer ride-matching problem in a flexible ridesharing system. Transportation Research Part B: Methodological 106, 218–236. https://doi.org/10.1016/j.trb.2017.10.006

Masoud, N., Lloret-Batlle, R., Jayakrishnan, R., 2017. Using bilateral trading to increase ridership and user permanence in ridesharing systems. Transportation Research Part E: Logistics and Transportation Review 102, 60–77. https://doi.org/10.1016/j.tre.2017.04.007

Meng, Q., Lam, W.H.K., Yang, L., 2008. General stochastic user equilibrium traffic assignment problem with link capacity constraints. Journal of Advanced Transportation 42, 429–465. https://doi.org/10.1002/atr.5670420403

Meng, Q., Liu, Z., Wang, S., 2014. Asymmetric stochastic user equilibrium problem with elastic demand and link capacity constraints, Transportmetrica A: Transport Science. https://doi.org/10.1080/23249935.2013.765929

Morency, C., 2007. The ambivalence of ridesharing. Transportation 34, 239–253. https://doi.org/10.1007/s11116-006-9101-9

Pang, J.-S., Facchinei, F., 2003. Finite-Dimensional Variational Inequalities and Complementarity Problems (I), Springer Series in Operations Research. https://doi.org/10.1007/b97543

Patriksson, M., 2015. The traffic assignment problem: models and methods. Courier Dover Publications.

RideGuru, 2018. The two biggest complaints we have with rideshares! [WWW Document]. URL https://ride.guru/content/newsroom/the-two-biggest-complaints-we-have-with-rideshares

Sheffi, Y., 1985. Urban Transportation Network, Pretince Hall.

Song, Z., Yin, Y., Lawphongpanich, S., 2015. Optimal Deployment of Managed Lanes in General Networks. International Journal of Sustainable Transportation 9, 431–441. https://doi.org/10.1080/15568318.2013.777263

Wang, J.P., Ban, X. (Jeff), Huang, H.J., 2019. Dynamic ridesharing with variable-ratio charging-compensation scheme for morning commute. Transportation Research Part B: Methodological 122, 390–415. https://doi.org/10.1016/j.trb.2019.03.006

Wang, X., Yang, H., Zhu, D., 2018. Driver-rider cost-sharing strategies and equilibria in a ridesharing program. Transportation Science 52, 868–881. https://doi.org/10.1287/trsc.2017.0801

Xiao L.L., Liu T.L., Huang H.J., 2016. On the morning commute problem with carpooling behavior under parking space constraint. Transportation Research Part B: Methodological 91, 383–407.

Xu, H., Pang, J.S., Ordóñez, F., Dessouky, M., 2015. Complementarity models for traffic equilibrium with ridesharing. Transportation Research Part B: Methodological 81, 161–182. https://doi.org/10.1016/j.trb.2015.08.013

Yan, C.-Y., Hu, M.-B., Jiang, R., Long, J., Chen, J.-Y., Liu, H.-X., 2019. Stochastic Ridesharing User Equilibrium in Transport Networks. Networks and Spatial Economics. https://doi.org/10.1007/s11067-019-9442-5

Yen, J.Y., 1971. Finding the K shortest loopless paths in a network. Management Science 17, 712–716. https://doi.org/10.1287/mnsc.17.11.712

Zhang, S., Yuan, R., Wu, Y., Yi, Y., 2017. Parallel computation of a dam-break flow model using OpenACC applications. Journal of Hydraulic Engineering 143, 1–10. https://doi.org/10.1061/(ASCE)HY.1943-7900.0001225

Appendix A: list of notations used throughout the study

Notations	Explanations
Sets:	
A	set of links, where $A = \{a\}$
I	set of roles, where $I = SD \cup RD \cup R = \{i\}$; $i \in SD$ denotes solo drivers; $i \in RD$ denotes ridesharing drivers; and $i \in R$ denotes riders
N	set of nodes, where $N = \{n\}$
P^w	set of paths between OD pairs w, where $P^w = \{p\}$
P	set of all paths, where $P = \bigcup_w P^w$
W	set of OD pairs, where $W = \{w\}$
Parameters:	

B_i^w	benchmark price (compensation) for riders (ridesharing driers) i between OD pair w
C	ridesharing capacity, $C = 4$ denotes one ridesharing drivers can pick up at most four riders
c_a, t_a^0	capacity and free-flow travel time of link a
q^w	travel demand between OD pair w
b, e	parameters used in BPR function
ρ_i, γ_i, m_i	value of time, inconvenience coefficient, and pricing coefficient for role i
$\delta_{a,p}^w$	link-path incidence parameter, where $\delta_{a,p}^{\omega} = 1$ if link a belongs to path p, otherwise $\delta_{a,p}^{\omega} = 0$
Variables:	
$C_{p,i}^{T,w}$, $C_i^{I,w}$, $C_i^{M,w}$	travel time, inconvenience and monetary cost of role i between OD pair w
$C_{p,i}^w$	travel cost function of role i on path p between OD pair w
$\tilde{C}_{p,i}^w$	generalized travel cost function of role i on path p between OD pair w
I_i	function of inconvenience cost for role i
R_i, C_i, M_i	functions used to calculate surge price or compensation for role i
$f_{p,i}^w$	path flow of role i on path p between OD pair w
t_a	travel time of link a
t_p^w	travel time of path p between OD pair w
$x_{a,i}$	link flow of role i on link a

Appendix B: number of paths between each OD pair

D / O	1	2	3	4	5	6	7	8	9	10	11	12	13	14	15	16	17	18	19	20	21	22	23	24
1	0	1	1	1	1	1	2	2	1	1	1	1	1	2	2	3	2	2	2	3	3	3	1	1
2	1	0	1	2	2	1	2	2	2	3	2	1	1	3	3	3	2	0	3	3	0	2	0	0
3	1	1	0	1	1	2	3	3	1	1	1	1	1	2	2	4	2	0	0	0	0	3	1	0
4	1	2	1	0	1	1	2	2	1	1	1	1	1	3	2	3	2	2	2	3	4	2	2	1
5	1	2	1	1	0	1	2	2	1	1	1	1	1	2	1	3	2	0	2	3	4	1	2	0
6	1	1	2	1	1	0	2	2	1	2	1	2	2	3	2	3	2	2	3	2	2	2	3	3
7	2	2	3	2	2	2	0	1	2	2	3	3	2	3	2	1	2	1	2	1	1	1	1	2
8	2	2	3	2	2	2	1	0	1	2	3	3	3	3	2	2	2	1	2	1	1	1	1	2
9	1	2	1	1	1	1	2	1	0	1	2	2	2	2	1	3	2	2	2	3	3	1	3	4
10	1	3	1	1	1	2	2	2	1	0	1	2	2	2	1	4	2	4	2	3	2	1	3	3
11	1	2	1	1	1	1	3	3	2	1	0	2	2	2	2	5	2	5	2	3	3	2	4	4
12	1	1	1	1	1	2	3	3	2	2	2	0	1	2	3	5	3	4	3	3	3	3	1	1
13	1	1	1	1	1	2	3	3	2	2	2	1	0	1	4	3	3	2	4	4	1	2	1	1
14	3	5	3	2	2	2	3	3	2	2	2	3	1	0	1	3	2	3	1	2	3	2	1	1

15	2	3	2	2	1	2	3	3	1	1	2	3	5	1	0	3	2	3	1	2	2	1	2	3
16	3	3	4	3	3	3	1	2	3	4	5	5	4	3	2	0	3	1	2	1	2	2	2	3
17	2	3	2	2	2	2	2	2	2	2	2	3	3	2	2	3	0	3	2	3	4	2	3	5
18	2	0	0	2	0	2	1	1	2	4	5	4	3	3	2	1	3	0	2	1	1	1	1	0
19	2	3	0	2	2	3	2	2	2	2	2	3	5	2	1	2	2	2	0	1	2	2	3	4
20	3	3	0	3	3	3	1	1	3	2	2	2	2	2	1	1	3	1	1	0	1	1	1	2
21	3	0	0	3	4	3	1	1	3	2	3	3	3	3	2	2	4	1	2	1	0	2	3	3
22	2	2	2	5	3	4	1	1	3	2	4	2	2	2	2	2	4	1	2	1	2	0	1	2
23	1	0	1	2	3	2	1	1	2	2	3	1	1	1	2	2	3	1	2	1	1	1	0	1
24	1	0	0	1	0	3	2	2	3	2	3	1	1	1	2	3	4	0	2	2	1	2	1	0